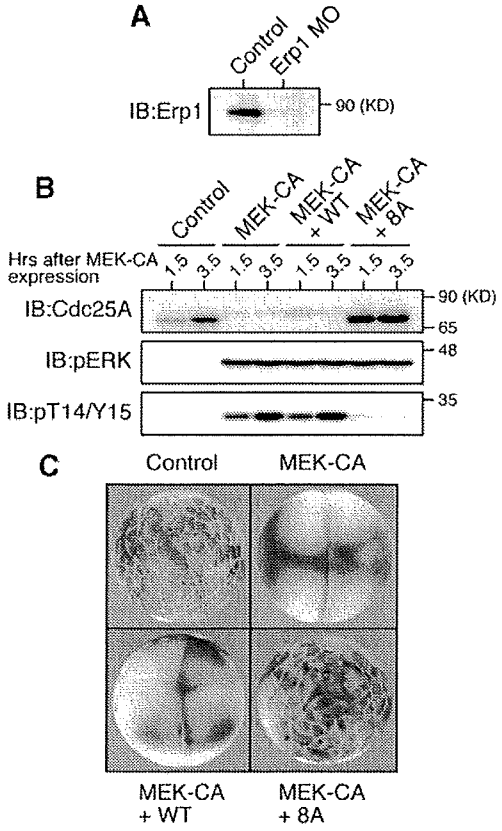

Figure 6. Cell cycle arrest in early embryos by ERK-induced Xe-Cdc25A degradation. (A) One-cell embryos 25 min after fertilization were injected with either water (Control) or 200 ng of Erp1 antisense morpholino oligos (Erp1-MO) and cultured for 1.5 h; embryo extracts were treated with λ-phosphatase and analyzed for endogenous Erp1 by immunoblotting. (B) One-cell embryos injected with Erp1 morpholino oligos as above were cultured for 35 min, injected with either water (Control), 5 ng of MEK-CA mRNA, or both 5 ng of MEK-CA mRNA and 200 pg of Myc-Xe-Cdc25A (WT or 8A) mRNA, cultured for the indicated times, and analyzed for Xe-Cdc25A (endogenous plus exogenous), phospho-ERK, and phospho-T14/Y15 by immunoblotting. (C) The embryos treated as in B were photographed 3 h after injection of MEK-CA mRNA (together with or without Myc-Xe-Cdc25A mRNA). Three and four independent experiments were performed for A and B, respectively, and, for each, a typical result is shown.

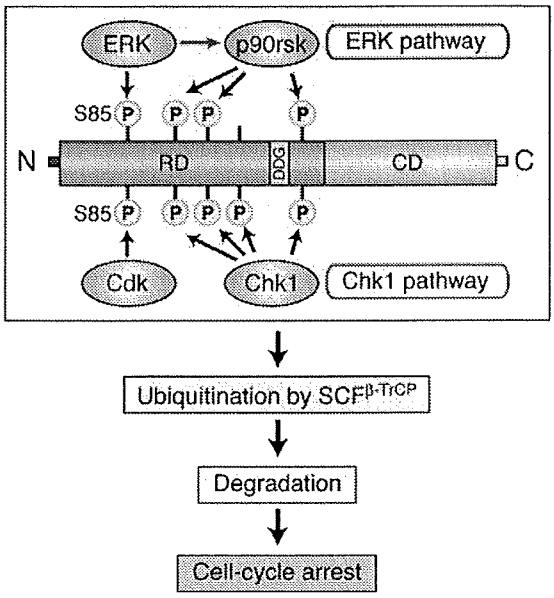

Figure 7. Model for the mechanism of Xe-Cdc25A degradation and cell cycle arrest induced by the ERK pathway. On strong activation of the ERK pathway, ERK phosphorylates Xe-Cdc25A on S85 (which normally is phosphorylated by Cdk) and other Ser residues (omitted), whereas the downstream kinase p90rsk phosphorylates Xe-Cdc25A on other multiple Ser residues (which overlap with Chk1 phosphorylation sites). These phosphorylations facilitate ubiquitination of Xe-Cdc25A by SCF$^{\beta\text{-TrCP}}$, thereby targeting the phosphatase for degradation and causing cell cycle arrest at interphase. For details, see text. RD, regulatory domain; DDG, DDG motif; CD, catalytic domain.

degradation involves the SCF$^{\beta\text{-TrCP}}$ ubiquitin ligase (Figure 1, C and D), similar to Chk1-induced degradation (Kanemori *et al.*, 2005). Furthermore, p90rsk, the kinase downstream of ERK, can phosphorylate Xe-Cdc25A on three of the four Chk1 phosphorylation sites (in the RXXS motifs) (Figure 2B) and thereby can target the phosphatase for degradation, albeit less efficiently than MEK (Figure 2C). Thus, it seems that the ERK pathway can induce Xe-Cdc25A degradation partly because p90rsk phosphorylates Xe-Cdc25A on sites overlapping with Chk1 phosphorylation sites (Figure 7). In this context, it is somewhat surprising that the p38 pathway, which has the Chk1-like kinase MK2 downstream of p38 (Manke *et al.*, 2005) and perhaps thereby targets mammalian Cdc25A for degradation under certain conditions (Khaled *et al.*, 2005; Reinhardt *et al.*, 2007), cannot efficiently induce Xe-Cdc25A degradation in eggs (Figure 1A). This is likely due, at least in part, however, to a relatively low abundance of MK2 protein in *Xenopus* eggs, because overexpression of MK2 (together with the p38 activator MKK6) can induce much more efficient degradation of Xe-Cdc25A in eggs (Supplemental Figure S3). Given our results and the structural analogy between the p38 and the ERK pathways (Raman *et al.*, 2007), MK2 may phosphorylate, at least in part, p90rsk phosphorylation sites, whereas p38 itself may phosphorylate ERK phosphorylation sites (see below), for Xe-Cdc25A degradation.

In addition to p90rsk, ERK itself also phosphorylates Xe-Cdc25A, but, in this case, on several SP motifs (Figure 3, A–D). This phosphorylation, as well as p90rsk phosphorylation (Figure 2A), is required, in part, for MEK-induced Xe-Cdc25A degradation (Figure 4, A and B). Double mutation of the ERK and p90rsk phosphorylation sites, however, renders Xe-Cdc25A (as well as human Cdc25A; Supplemental Figure S2) nearly completely resistant to MEK-induced degradation (Figure 4C). Thus, it seems that ERK phosphorylation and p90rsk phosphorylation contribute, roughly equally and additively, to the MEK-induced degradation of Xe-Cdc25A (as well as of human Cdc25A) (Figure 7). Interestingly, however, S85, the most important ERK phosphorylation site (Figure 4A), is also phosphorylated by Cdk (perhaps Cdk2; Ducruet and Lazo, 2003) in eggs (Figure 3, D and E), although this phosphorylation (by Cdk) is not required for ERK-induced Xe-Cdc25A degradation (because of its phosphorylation by ERK itself) (Figure 3E and Supplemental Figure S1A). Notably, S85 and phosphorylation of its equivalent site S88 are required, in part, for the Chk1-induced degradations of Xe-Cdc25A and human Cdc25A, respectively (Busino *et al.*, 2003; Kanemori *et al.*, 2005), and

Cdk activity is required for Chk1-induced Xe-Cdc25A degradation (our unpublished data). Therefore, S85 of Xe-Cdc25A (as well as S88 of human Cdc25A) is probably phosphorylated by Cdk in the case of Chk1-induced degradation (Figure 7).

How might phosphorylation of the RXXS and SP motifs (by p90rsk and ERK, respectively) act to target Xe-Cdc25A for $SCF^{\beta\text{-}TrCP}$-dependent degradation? This question is important because both the RXXS and SP motifs are located dispersedly far from the DDG motif (to which β-TrCP binds) (Figure 7). Concerning this issue, our preliminary experiments suggested that, whereas the phosphorylation of the RXXS and SP motifs is not necessarily required for β-TrCP binding of Xe-Cdc25A upon ERK activation, it is required significantly for efficient ubiquitination of the phosphatase (data not shown). (This contrasts with the case of human Wee1, in which Cdk phosphorylation of an SP motif near the DDG-like motif promotes both β-TrCP binding and ubiquitination; Watanabe *et al.*, 2005). Thus, it is conceivable that phosphorylation of the RXXS/SP motifs might act to facilitate ubiquitination of Xe-Cdc25A by the bound $SCF^{\beta\text{-}TrCP}$, perhaps by causing conformational changes of the phosphatase (Figure 7). A similar role has been suggested for Chk1-phosphorylated RXXS motifs in both human Cdc25A and Xe-Cdc25A (Busino *et al.*, 2003; Kanemori *et al.*, 2005).

The ERK pathway can target (ectopic) Xe-Cdc25A for $SCF^{\beta\text{-}TrCP}$-dependent degradation even under physiological conditions, or during oocyte maturation, in which the endogenous ERK pathway is fully activated (Figure 5). This result could explain the mechanism for degradation of endogenous Cdc25A during mouse oocyte maturation, which has recently been shown to occur and to be important for meiotic progression of the oocyte (Solc *et al.*, 2008).

Importantly, we find that strong ERK activation can induce cell cycle arrest in early embryos by targeting Xe-Cdc25A for degradation (Figure 6; also see Figure 7). This finding can explain why activating ERK early in cycling egg extracts can cause a G2 arrest (Walter *et al.*, 1997; Bitangcol *et al.*, 1998; Murakami and Vande Woude, 1998). Furthermore, our finding seems to have an important implication in the effects of strongly activated ERK on somatic cells. As is well known, whereas weak or sustained ERK activation is generally mitogenic, strong ERK activation by oncogenic Ras or activated Raf leads to cell cycle arrest in many cell types (and also differentiation in some cases) (Ebisuya *et al.*, 2005; Meloche and Pouyssegur, 2007). This cell cycle arrest may be elicited and maintained primarily by the ERK-induced expression of Cdk inhibitors, such as $p21^{Cip1}$ and $p16^{Ink4a}$ (Pumiglia and Decker, 1997; Serrano *et al.*, 1997; Zhu *et al.*, 1998). Given our results and the degradation of Cdc25A in TPA-treated human cells (Supplemental Figure S4); however, such cell cycle arrest could also be contributed to by an ERK-induced degradation of Cdc25A, similar to cell cycle arrest by Chk1-induced Cdc25A degradation (Donzelli and Draetta, 2003; Bartek and Lukas, 2003). The Ras/Raf- or ERK-induced cell cycle arrest is followed by senescence, a cellular response currently considered to be a defense against neoplasmic transformation (Serrano *et al.*, 1997; Zhu *et al.*, 1998). Thus, degradation of Cdc25A, together with the expression of Cdk inhibitors, might act as a fail-safe mechanism to limit the well-known transforming potential of excessive ERK mitogenic signaling (Lin *et al.*, 1998). In any case, our results suggest that the ERK pathway, when strongly activated, negatively influences cell cycle progression by targeting Cdc25A for $SCF^{\beta\text{-}TrCP}$-dependent degradation.

ACKNOWLEDGMENTS

We thank members of the Sagata laboratory for discussions and K. Gotoh for typing the manuscript. This work was supported by grants from the CREST Research Project of the Japan Science and Technology Agency and from the Ministry of Education, Culture, Sports, Science and Technology of Japan (to N. S.).

REFERENCES

Alonso, G., Ambrosino, C., Jones, M., and Nebreda, A. R. (2000). Differential activation of p38 mitogen-activated protein kinase isoforms depending on signal strength. J. Biol. Chem. *275*, 40641–40648.

Bartek, J., and Lukas, J. (2003). Chk1 and Chk2 kinases in checkpoint control and cancer. Cancer Cell *3*, 421–429.

Bitangcol, J. C., Chau, A.S.S., Stadnick, E., Lohka, M. J., Dicken, B., and Shibuya, E. K. (1998). Activation of the p42 mitogen-activated protein kinase pathway inhibits Cdc2 activation and entry into M-phase in cycling *Xenopus* egg extracts. Mol. Biol. Cell *9*, 451–467.

Busino, L., Donzelli, M., Chiesa, M., Guadavaccaro, D., Ganoth, D., Dorrello, N. V., Hershko, A., Pagano, M., and Draetta, G. F. (2003). Degradation of Cdc25A by β-TrCP during S phase and in response to DNA damage. Nature *426*, 87–91.

Donzelli, M., and Draetta, G. F. (2003). Regulating mammalian checkpoints through Cdc25 inactivation. EMBO Rep. *4*, 671–677.

Ducruet, A. P., and Lazo, J. S. (2003). Regulation of Cdc25A half-life in interphase by cyclin-dependent kinase 2 activity. J. Biol. Chem. *278*, 31838–31842.

Ebisuya, M., Kondoh, K., and Nishida, E. (2005). The duration, magnitude and compartmentalization of ERK MAP kinase activity: mechanisms for providing signaling specificity. J. Cell Sci. *118*, 2997–3002.

Frescas, D., and Pagano, M. (2008). Deregulated proteolysis by the F-box proteins SKP2 and β-TrCP: tipping the scales of cancer. Nat. Rev. Cancer *8*, 438–449.

Frodin, M., and Gammeltoft, S. (1999). Role and regulation of 90 kDa ribosomal S6 kinase (RSK) in signal transduction. Mol. Cell. Endocrinol. *151*, 65–77.

Hoffmann, I., Draetta, G., and Karsenti, E. (1994). Activation of the phosphatase activity of human cdc25A by a cdk2-cyclin E dependent phosphorylation at the G_1/S transition. EMBO J. *13*, 4302–4310.

Inoue, D., Ohe, M., Kanemori, Y., Nobui, T., and Sagata, N. (2007). A direct link of the Mos-MAPK pathway to Erp1/Emi2 in meiotic arrest of *Xenopus laevis* eggs. Nature *446*, 1100–1104.

Jin, J., Shirogane, T., Xu, L., Nalepa, G., Qin, J., Elledge, S. J., and Harper, J. W. (2003). $SCF^{\beta\text{-}TRCP}$ links Chk1 signaling to degradation of the Cdc25A protein phosphatase. Genes Dev. *17*, 3062–3074.

Kanemori, Y., Uto, K., and Sagata, N. (2005). β-TrCP recognizes a previously undescribed nonphosphorylated destruction motif in Cdc25A and Cdc25B phosphatases. Proc. Natl. Acad. Sci. USA *102*, 6279–6284.

Khaled, A. R., Bulavin, D. V., Kittipatarin, C., Li, W. Q., Alvarez, M., Kim, K., Young, H. A., Fornace, A. J., and Durum, S. K. (2005). Cytokine-driven cell cycling is mediated through Cdc25A. J. Cell Biol. *169*, 755–763.

Kim, S.H.Li.C., and Maller, J. L. (1999). A maternal form of the phosphatase Cdc25A regulates early embryonic cell cycles in *Xenopus laevis*. Dev. Biol. *212*, 381–391.

Kishimoto, T. (2003). Cell cycle control during meiotic maturation. Curr. Opin. Cell Biol. *15*, 654–663.

Lei, K., Nimnual, A., Zong, W. X., Kennedy, N. J., Flavell, R. A., Thompson, C. B., Bar-Sagi, D., and Davis, R. J. (2002). The Bax subfamily of Bcl2-related proteins is essential for apoptotic signal transduction by c-Jun NH(2)-terminal kinase. Mol. Cell. Biol. *22*, 4929–4942.

Lin, A. W., Barradas, M., Stone, J. C., van Aelst, L., Serrano, M., and Lowe, S. W. (1998). Premature senescence involving p53 and p16 is activated in response to constitutive MEK/MAPK mitogenic signaling. Genes Dev. *12*, 3008–3019.

Mailand, N., Falck, J., Lukas, C., Syljuåsen, R. G., Welcker, M., Bartek, J., and Lukas, J. (2000). Rapid destruction of human Cdc25A in response to DNA damage. Science *288*, 1425–1429.

Manke, I. A., Nguyen, A., Lim, D., Stewart, M. Q., Elia, A. E., and Yaffe, M. B. (2005). MAPKAP kinase-2 is a cell cycle checkpoint kinase that regulates the G2/M transition and S phase progression in response to UV irradiation. Mol. Cell *17*, 37–48.

Mansour, S. J., Matten, W. T., Hermann, A. S., Candia, J. M., Rong, S., Fukasawa, K., Vande Woude, G. F., and Ahn, N. G. (1994). Transformation of mammalian cells by constitutively active MAP kinase kinase. Science *265*, 966–970.

Meloche, S., and Pouyssegur, J. (2007). The ERK1/2 mitogen-activated protein kinase pathway as a master regulator of the G1- to S-phase transition. Oncogene *26*, 3227–3239.

Molinari, M., Mercurio, C., Dominguez, J., Goubin, F., and Draetta, G. F. (2000). Human Cdc25A inactivation in response to S phase inhibition and its role in preventing premature mitosis. EMBO Rep., *1*, 71–79.

Muda, M., Theodosiou, A., Rodrigues, N., Boschert, U., Camps, M., Gillieron, C., Davies, K., Ashworth, A., and Arkinstall, S. (1996). The dual specificity phosphatases M3/6 and MKP-3 are highly selective for inactivation of distinct mitogen-activated protein kinases. J. Biol. Chem. *271*, 27205–27208.

Murakami, M. S., and Vande Woude, G. F. (1998). Analysis of the early embryonic cell cycles of *Xenopus*; regulation of cell cycle length by Xe-wee1 and Mos. Development *125*, 237–248.

Nishiyama, T., Ohsumi, K., and Kishimoto, T. (2007). Phosphorylation of Erp1 by p90rsk is required for cytostatic factor arrest in *Xenopus laevis* eggs. Nature, *446*, 1096–1099.

Okamoto, K., and Sagata, N. (2007). Mechanism for inactivation of the mitotic inhibitory kinase Wee1 at M phase. Proc. Natl. Acad. Sci. USA *104*, 3753–3758.

Pumiglia, K. M., and Decker, S. J. (1997). Cell cycle arrest mediated by the MEK/mitogen-activated protein kinase pathway. Proc. Natl. Acad. Sci. USA *94*, 448–452.

Raman, M., Chen, W., and Cobb, M. H. (2007). Differential regulation and properties of MAPKs. Oncogene *26*, 3100–3112.

Reinhardt, H. C., Aslanian, A. S., Lees, J. A., and Yaffe, M. B. (2007). p53-deficient cells rely on ATM- and ATR-mediated checkpoint signaling through the p38MAPK/MK2 pathway for survival after DNA damage. Cancer Cell *11*, 175–189.

Sagata, N. (1997). What does Mos do in oocytes and somatic cells? Bioessays *19*, 13–21.

Serrano, M., Lin, A. W., McCurrach, M. E., Beach, D., and Lowe, S. W. (1997). Oncogenic *ras* provokes premature cell senescence associated with accumulation of p53 and p16INK4a. Cell *88*, 593–602.

Shimuta, K., Nakajo, N., Uto, K., Hayano, Y., Okazaki, K., and Sagata, N. (2002). Chk1 is activated transiently and targets Cdc25A for degradation at the *Xenopus* midblastula transition. EMBO J. *21*, 3694–3703.

Solc, P., Saskova, A., Baran, V., Kubelka, M., Schultz, R. M., and Motlik, J. (2008). CDC25A phosphatase controls meiosis I progression in mouse oocytes. Dev. Biol. *317*, 260–269.

Sturgill, T. M., Ray, L. B., Erikson, E., and Maller, J. L. (1988). Insulin-stimulated MAP-2 kinase phosphorylates and activates ribosomal protein S6 kinase II. Nature *334*, 715–718.

Uto, K., Inoue, D., Shimuta, K., Nakajo, N., and Sagata, N. (2004). Chk1, but not Chk2, inhibits Cdc25 phosphatases by a novel common mechanism. EMBO J. *23*, 3386–3396.

Walter, S. A., Guadagno, T. M., and Ferrell,, J. E., Jr. (1997). Induction of a G_2-phase arrest in *Xenopus* egg extracts by activation of p42 mitogen-activated protein kinase. Mol. Biol. Cell. *8*, 2157–2169.

Yamanaka, H., Moriguchi, T., Masuyama, N., Kusakabe, M., Hanafusa, H., Takeda, R., Takeda, S., and Nishida, E. (2002). JNK functions in the non-canonical Wnt pathway to regulate convergent extension movements in vertebrates. EMBO Rep. *3*, 69–75.

Watanabe, N., Arai, H., Iwasaki, J. -I., Shiina, M., Ogata, K., Hunter, T., and Osada, H. (2005). Cyclin-dependent kinase (CDK) phosphorylation destabilizes somatic Wee1 via multiple pathways. Proc. Natl. Acad. Sci. USA *102*, 11663–11668.

Zhu, J., Woods, D., McMahon, M., and Bishop, J. M. (1998). Senescence of human fibroblasts induced by oncogenic Raf. Genes Dev. *12*, 2997–3007.

Cancer Gene Therapy (2009) 16, 126–136

www.nature.com/cgt

ORIGINAL ARTICLE

E1A, E1B double-restricted replicative adenovirus at low dose greatly augments tumor-specific suicide gene therapy for gallbladder cancer

K Fukuda[1], M Abei[1], H Ugai[2,4], R Kawashima[1,2], E Seo[1], M Wakayama[1], T Murata[2], S Endo[1], H Hamada[3], I Hyodo[1] and KK Yokoyama[2]

[1]*Division of Gastroenterology, Graduate School of Comprehensive Human Sciences, University of Tsukuba, Tsukuba, Ibaraki, Japan;* [2]*Division of Gene Engineering, BioResource Center, Institute of Physical and Chemical Research, RIKEN, Tsukuba, Ibaraki, Japan and* [3]*Department of Molecular Medicine, Sapporo Medical University, Sapporo, Hokkaido, Japan*

Combination therapy with replicative oncolytic viruses is a recent topic in innovative cancer therapy, but few studies have examined the efficacy of oncolytic adenovirus plus replication-deficient adenovirus carrying a suicide gene. We aim to evaluate whether an E1A, E1B double-restricted oncolytic adenovirus, AxdAdB-3, can improve the efficacy for gallbladder cancers (GBCs) of the replication-deficient adenovirus-based herpes simplex virus thymidine kinase (HSVtk)/ganciclovir (GCV) therapy directed by the carcinoembryonic antigen (CEA) promoter. Cytopathic effects of AxdAdB-3 plus AxCEAprTK (an adenovirus expressing *HSVtk* directed by CEA promoter) or AxCAHSVtk (an adenovirus expressing *HSVtk* directed by a nonspecific CAG promoter) with GCV administration were examined in several GBC lines and normal cells. Efficacy *in vivo* was tested in severe combined immunodeficiency disease mice with GBC xenografts. Addition of AxdAdB-3 (1 multiplicity of infection, MOI) significantly enhanced the cytopathic effects of AxCEAprTK (10 MOI)/GCV on GBC cells. The augmented effect was attributable to the replication of the AxCEAprTK and also to the enhanced CEA promoter activity, which was presumably transactivated by E1A. In normal cells, AxdAdB-3 (20 MOI) plus AxCEAprTK (200 MOI)/GCV was not cytopathic, whereas AxdAdB-3 (1 MOI) plus AxCAHSVtk (10 MOI)/GCV was significantly toxic. Low-dose AxdAdB-3 (2×10^7 PFU, plaque-forming unit) plus AxCEAprTK (2×10^8 PFU)/GCV significantly suppressed the growth of GBC xenografts as compared with either AxdAdB-3 (2×10^7 PFU)/GCV or AxCEAprTK (2×10^9 PFU)/GCV alone. E1A, E1B double-restricted replicating adenovirus at low dose significantly augmented the efficacy of CEA promoter-directed HSVtk/GCV therapy without obvious toxicity to normal cells, suggesting a potential use of this combination for treating GBC and other CEA-producing malignancies.
Cancer Gene Therapy (2009) **16**, 126–136; doi:10.1038/cgt.2008.67; published online 26 September 2008

Keywords: suicide gene; adenovirus; gallbladder cancer; carcinoembryonic antigen

Introduction

Gallbladder cancer (GBC) is the fifth most common gastrointestinal malignancy, and its incidence in the United States and in Japan is 2.5 and 10 per 100 000 persons, respectively.[1] The disease is only curable at its early stages, but only approximately 30% of patients undergo curative surgery.[1,2] Other currently available treatments also have little effect on advanced GBC and the 5-year survival rate is only about 5% in such cases.[1,2] Therefore, a new treatment modality, such as gene therapy, merits a high priority, but few studies are available for GBCs.

Gene-directed enzyme prodrug therapy (GDEPT), also known as suicide gene therapy, using the herpes simplex virus thymidine kinase gene (HSVtk)/ganciclovir (GCV) system delivered by replication-defective viral vectors has been studied extensively as a first-generation gene therapy approach for various cancers. Tissue- or tumor-specific promoters have been used to limit the expression of suicide genes to cancer cells specifically.[3–7] Gastrointestinal malignancies including GBC often produce carcinoembryonic antigen (CEA) at high levels.[8] When suicide genes were placed under the control of the CEA promoter in the vectors, the specificity and safety of suicide gene

Correspondence: Dr M Abei, Division of Gastroenterology, Graduate School of Comprehensive Human Sciences, University of Tsukuba, 1-1-1 Tennoudai, Tsukuba, Ibaraki 305-8575, Japan.
E-mail: m-abei@md.tsukuba.ac.jp
[4]Present address: H Ugai, Gene Therapy Center, University of Alabama at Birmingham, Birmingham, AL, USA.
Received 23 March 2008; revised 6 July 2008; accepted 31 July 2008; published online 26 September 2008

therapy for CEA-producing cancers was enhanced.[3–6] However, this approach had two limitations: the activity of the CEA promoter as the promoter of therapeutic transgenes is significantly lower than that of nonspecific promoters, such as the chicken β-actin enhancer β-globin promoter (CAG) promoter,[9–11] and the efficiency of gene delivery is limited because of the use of nonreplicating vectors.

By contrast, conditionally replicative adenoviruses (CRAds), which are capable of cancer-selective replication and oncolysis, have recently received widespread attention as a strategy for innovative cancer therapy (12–23; for reviews see references 12–14). For instance, ONYX-015, which lacks a p53-binding E1B-55 kDa protein and replicates efficiently in tumor cells that lack p53-dependent functions and its clinical trails of in combination with chemotherapy, have yielded remarkably good efficacy and safety in patients with head and neck cancers.[14,15] Another CRAds with a mutation in the retinoblastoma protein (pRb)-binding domain of E1A have been shown to replicate in tumor cells with disrupted Rb signaling pathway.[16,17] Although these single-mutated CRAds exhibited potential for cancer therapy, these viruses do replicate and cause some cytopathic effects (CPEs) in normal cells *in vitro*.[16,18,19] Moreover, the clinical trial of intralesional ONYX-015 in patients with hepatobiliary cancers showed sufficient safety but limited therapeutic effects.[20,21] These studies suggest that further efforts are necessary to enhance the antitumor activity still further.

Therefore, recent studies have focused on developing and optimizing the combination therapy of oncolytic viruses with other therapeutic modalities including suicide genes or genes for cytokines.[24–33] Most attempts to combine CRAds with GDEPT used a single 'armed' CRAd, in which the CRAd was armed with a suicide gene, but the results have been inconsistent.[26–33] Only few studies have explored the efficacy of two-vector systems and no studies have examined the combination of a CRAd and a replication-defective adenovirus (Ad)-expressing suicide gene driven by a tumor-specific promoter.

We have previously introduced AxdAdB-3, a novel CRAd which has mutations in both *E1A* and *E1B*.[22] We demonstrated that the double-mutant CRAd had potent oncolytic activities to biliary cancers with an enhanced safety profile to human normal cells than the ONYX-015-type E1B single-restricted CRAd.[22] A similar double-mutant CRAd has also been shown by others to exhibit efficacy for glioma cells with a highly attenuated replication in normal astrocytes.[23] The enhanced safety profile of the double-mutant CRAd may allow more effective treatment by combining with other therapeutic modalities.

In the present study, we examined the efficacy and safety of the combination of the E1A, E1B double-mutant CRAd (AxdAdB-3) and a replication-defective Ad vector that carried a CEA promoter-driven *HSVtk* gene (AxCEAprTK) followed by GCV treatment. We compared the results with the efficacy of each monotherapy and of the combination of AxdAdB-3 and a nonreplicative Ad vector in which the *HSVtk* gene was driven by a nonspecific CAG promoter (AxCAHSVtk) followed by GCV treatment. Our results revealed that the antitumor effects of AxCEAprTK/GCV were greatly augmented by a low dose of AxdAdB-3. We attributed the augmentation to the increased expression of the suicide gene because coinfected AxdAdB-3 enabled the replication-defective vector to proliferate, and also, increased the activity of the CEA promoter, presumably throughtransactivation by Ad E1A. In addition, the combination exhibited enhanced safety, in terms of its effects on normal cells, as compared to the combination of AxCAHSVtk and AxdAdB-3. These results suggests the efficacy of this approach especially for the treatment of GBC, which is characterized both by high rates of abnormalities in p53 and Rb pathways[34–38] and by a high incidence of CEA production.[39]

Materials and methods

Cell lines and culture

A GBC cell line, TGBC-44TKB, was established by Dr T Todoroki (Division of Surgery, University of Tsukuba, Ibaraki, Japan) and another GBC line, Mz-ChA2, was provided by Dr A Knuth (Johannes-Gutenberg University, Mainz, Germany). These two lines of GBC cells, HeLa (cervical carcinoma) cells and WI-38 (human fibroblasts) cells were maintained in Dulbecco's modified Eagle's medium (DMEM) supplemented with 10% fetal bovine serum. Primary cultures of human intestinal epithelial cells (referred to here as epithelial cells) were purchased from the Applied Cell Biology Research Institute (Kirkland, WA). They were cultured on culture plates that had been coated with type I collagen (Iwaki, Tokyo, Japan) and were maintained in CS-2.0 complete serum-free medium (Cell Systems, Kirkland, WA). Human embryonic kidney 293 cells (HEK293 cells) were purchased from the American Type Culture Collection (Manassas, VA).

Viral vectors

Generation of AxdAdB-3 was described previously.[22] Briefly, a mutant *Ad5 E1A* gene fragment containing a STGHE (S × G × E) mutation at the LTCHE (L × C × E) Rb-binding pocket motif in the Ad5 E1A exon 1, was obtained by reverse transcriptase (RT)–PCR.[22] AxdAdB-3 has the E1A with S × G × E (STGHE) mutation (dA) together with the E1B 55 K mutation (dB; reference 40). Recombinant Ads, namely, AxCEAprTK,[5] which carries a gene for *HSVtk* directed by a CEA promoter, AxCEAprZ,[4] which carries a *LacZ* gene directed by a CEA promoter; AxCAHSVtk, which carries a *HSVtk* gene directed by a CAG promoter; AxCALacZ, which carries a *LacZ* gene directed by CAG promoter; and Axlwl (mock), which is an Ad with deleted E1 and E3 regions, were provided by the RIKEN DNA Bank (Tsukuba, Ibaraki, Japan) and their construction was described previously.[4] All Ads were purified by CsCl gradient centrifugation. Titers of Ads were evaluated by the standard plaque-forming assay with HEK293 cells.

CPEs in vitro

GBC cells and normal cells were seeded in 96-well culture plates, at a density of 2×10^3 cells per well, and infected with Ads. The CPEs of the vectors were assessed 3 and 6 days after infection by the colorimetric WST-1 assay (Takara, Otsu, Shiga, Japan).[22] WST-1, a tetrazolium salt, is cleaved to yield a formazan product by enzymes in metabolically active cells, and the reaction is quantitated with an automatic plate reader at 450 nm with a reference wavelength of 650 nm. Under the experimental conditions of the present study, there was a direct correlation between the absorbance at 450 nm and the number of viable cells determined by light microscopy.[22] Each result was expressed as a percentage of the absorbance of control (uninfected) cells.

Qualitative and quantitative assessment of CEA promoter-directed transgene expression

For qualitative assessment of the CEA promoter-directed transgene expression, we infected cells with AxCEAprZ at a multiplicity of infection (MOI) of 10 or 100. Then, 24 h after infection, the cells were fixed in phosphate-buffered saline (PBS; 10.9 mM Na_2HPO_4, 1.8 mM NaH_2PO_4, 8.2 g l^{-1} NaCl) that contained 0.25% glutaraldehyde for 10 min at 4 °C, and stained with X-gal solution (1 mg ml^{-1} 5-bromo-4-chloro-3-indolyl-β-galactopyranoside, 5 mM $K_4Fe(CN)_6$, 5 mM $K_3(CN)_6$, and 2 mM $MgCl_2$ in PBS) for 3 h at 37 °C. Cells with CEA promoter activity were identified by blue staining of nuclei. To evaluate the effects of coinfection with AxdAdB-3, we simultaneously coinfected cells with Ax-CEAprZ at 10 MOI and AxdAdB-3 at 1 MOI. After incubation for 72 h, cells were stained with X-gal.

For the quantitative assessment of the CEA promoter-directed transgene expression, we infected cells with AxCEAprZ (100 MOI) and AxdAdB-3 or Axlwl at 0, 1, 10 or 100 MOI. In order to reduce the effects of the replication of AxCEAprZ, we assayed cells 10 h later. Harvested cells were lysed and centrifuged for preparation of both a supernatant and a DNA fraction. The β-galactosidase activity in the supernatant was assayed with a β-Gal Assay Kit (Invitrogen Corp., Carlsbad, CA) in which the amount of *o*-nitrophenyl hydrolyzed from *o*-nitrophenyl-β-D-galactopyranoside by β-galactosidase was quantitated at 420 nm. To evaluate the proliferation of AxCEAprZ simultaneously, we measured the number of copies of the AxCEAprZ genome in the DNA fraction by quantitative PCR using SYBRGreen PCR Master Mix and RT–PCR (Applied Biosystems, Foster City, CA) according to the manufacturer's instructions. The *LacZ* gene was targeted for amplification using primers LacZ no. F1 (taactcggcgtttcatctgt) and LacZ no. R1 (taaaaatgcgctcaggtcaaatt).

Plasmids and effects of Ad E1A co-transfection on CEA promoter activity

We examined the effects of Ad E1A.13S. on the activity of CEA promoter in plasmid co-transfection experiments. Plasmid pGL3-CEApr, which carries the gene for firefly luciferase directed by the CEA promoter was provided by the RIKEN DNA Bank (Tsukuba, Ibaraki, Japan) and plasmid pE1A5.13S,[41] which carries the *E1A-13S* gene of Ad type 5, was provided by Dr Shiroki (Tokyo University, Tokyo, Japan). Plasmid pSV-β-galactosidase, which carries a gene for β-galactosidase directed by the senminum virus 40 promoter; plasmid phRL-TK, which carries the gene for Renilla luciferase; and plasmid pGL3-basic, which carries the gene for firefly luciferase were purchased from Promega (Madison, WI).

We co-transfected TGBC-44TKB and Mz-ChA2 cells using Lipofectamine 2000 (Invitrogen Corp.) with pGL3-CEApr (0.5 μg) and phRL-TK (0.1 μg), plus a total of 1.0 μg of pSVE1A13S and pSV-β-galactosidase at different dose ratios, and then we measured the activity of the CEA promoter in the cells by a dual-luciferase assay. Transfected cells were lysed 24 h after transfection and assayed for luciferase activity with a Dual-Luciferase Reporter Assay System (Promega) according to the manufacturer's instructions. In control experiments, pGL3-basic (0.5 μg) was used instead of pGL3-CEApr.

Animal studies

Female, 4-week old, severe combined immunodeficiency disease (SCID) mice (C.B-17/lcr-scid. jcl; CLEA Japan, Tokyo, Japan) were quarantined for 1 week. A subcutaneously (s.c.) GBC xenograft model was prepared by injecting s.c. 1×10^7 TGBC-44TKB cells in 100 μl of DMEM, without serum, into the left flank of each mouse. Tumors were measured with calipers and the volume was calculated as 0.4 × longest diameter × width^2. When the tumors had reached approximately 50–80 mm^3 (a diameter of 5–6 mm), animals (a total of 36) were assigned randomly to the following six groups: (1) intratumorally (i.t.) injection of AxCEAprTK (2×10^9 PFU, plaque-forming unit) in PBS (100 μl) with GCV (200 mg kg^{-1}) (classical suicide gene treatment; $n = 6$); (2) i.t. injection of AxCEAprTK (2×10^8 PFU) and AxdAdB-3 (2×10^7 PFU) in PBS (100 μl) with GCV (200 mg kg^{-1}) (combination suicide gene treatment; $n = 6$); (3) i.t. injection of AxCEAprTK (2×10^8 PFU) and AxdAdB-3 (2×10^7 PFU) in PBS (100 μl) without GCV ($n = 6$); (4) i.t. injection of AxdAdB-3 (2×10^7 PFU) in PBS (100 μl) with GCV (200 mg/kg) ($n = 6$); (5) i.t. injection of PBS (100 μl) alone ($n = 6$); and (6) GCV (200 mg/kg) alone ($n = 6$). Vectors were injected i.t. on day 1, and GCV was injected intraperitoneally (i.p.) on days 4 through 8. All mice received human care in compliance with the guidelines for the care and use of laboratory animals in research.

Statistical analysis

The results of the WST-1 assay, the β-galactosidase assay, the dual-luciferase assay and the volumes of tumors are presented as mean ± s.d. The significance of differences between groups was assessed by Student's unpaired two-tailed *t*-test.

Results

Effects of CEA-promoter-directed HSVtk/GCV treatment on GBC and normal cells

We first examined the activity of the CEA promoter in two lines of GBC cells (TGBC-44TKB and Mz-ChA2), as

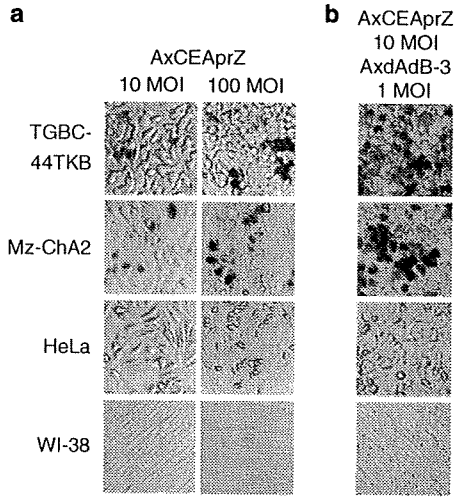

Figure 1 Carcinoembryonic antigen (CEA) promoter-directed transgene (*LacZ*) expression following infection with AxCEAprZ with or without combination with AxdAdB-3 in gallbladder cancer (GBC), HeLa and WI-38 cells. In order to evaluate the CEA promoter-directed transgene expression in GBC cells, GBC, HeLa and WI-38 cells were infected with AxCEAprZ (10 or 100 multiplicity of infection, MOI) alone or with AxCEAprZ (10 MOI) plus AxdAdB-3 (1 MOI), and stained with X-gal 24 h (**a**) or 72 h (**b**) later.

well as in HeLa, and WI-38 (normal fibroblast) cells (Figure 1). The number of cells stained with X-gal increased dose dependently in the two lines of GBC cells after infection with AxCEAprZ, suggesting that the CEA promoter was very active in these cells. By contrast, minimal staining was detected in HeLa and WI-38 cells, suggesting that the CEA promoter was inactive in these cells (Figure 1a; see below for explanation of Figure 1b).

We then examined the extent and specificity of the CPE of AxCEAprTK/GCV, namely, the CEA promoter-directed HSVtk/GCV suicide gene treatment, in a comparison with those of AxCAHSVtk/GCV, namely, the suicide gene therapy directed by a nonspecific CAG promoter (Figure 2). Cells were infected with AxCEAprTK or AxCAHSVtk at 10 or 100 MOI and exposed to GCV (20 $\mu g\,ml^{-1}$) from day 3 through 6. AxCAHSVtk/GCV had a potent CPE on all cell lines and the effects were dose dependent. By contrast, AxCEAprTK/GCV had only a moderate CPE on the two lines of GBC cells, and no clear CPE on HeLa and WI-38 cells (Figure 2). The CPE of AxCEAprTK/GCV on the GBC cells was lower than that of AxCAHSVtk/GCV. GCV alone did not have any CPE on these cell lines (data not shown). These results confirmed that the use of the CEA promoter limited the CPE of GCV exclusively to the cells in which the CEA promoter was very active, and that the CPE of AxCEAprTK (10 MOI)/GCV was relatively weak.

Effects of combination with AxdAdB-3 on the CEA-promoter-directed HSVtk/GCV treatment in GBC and normal cells

We then examined whether coinfection with AxdAdB-3 could increase the CEA promoter-directed transgene expression. The staining with X-gal of the two lines of

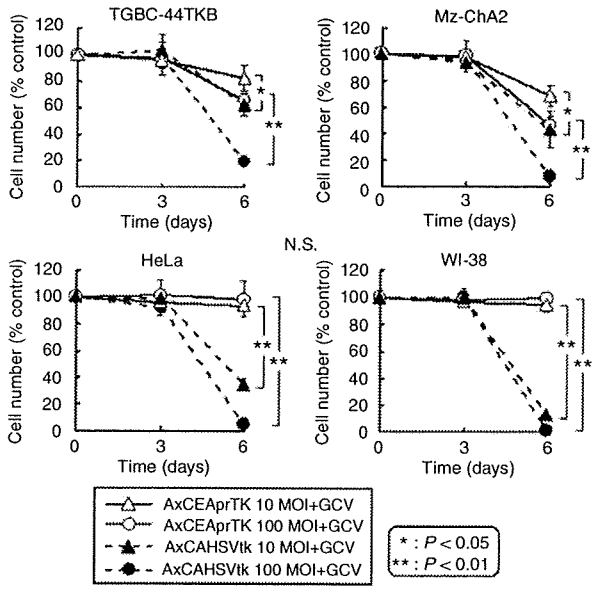

Figure 2 Cytopathic effects of carcinoembryonic antigen (CEA) promoter-directed and nonspecific promoter-directed herpes simplex virus thymidine kinase (HSVtk)/ganciclovir (GCV) suicide gene treatment of gallbladder cancer (GBC), HeLa and WI-38 cells. In order to evaluate the potency and specificity of the cytopathic effect (CPE) of CEA promoter-directed HSVtk/GCV treatment, cells were infected with AxCEAprTK or AxCAHSVtk at a multiplicity of infection (MOI) of 10 and 100, and they were exposed to GCV (20 $\mu g\,ml^{-1}$) 3 days later. The graphs show changes with time in numbers of viable cells (% control) as assessed by the WST-1 assay. Values are presented as means ± s.d. Statistically significant differences in terms of the CPE between AxCEAprTK/GCV and AxCAHSVtk/GCV at the same MOI are indicated by $^{**}P<0.01$ or $^{*}P<0.05$.

GBC cells after infection with AxCEAprZ (10 MOI) plus AxdAdB-3 (1 MOI) was even more intense and extensive than that after infection with AxCEAprZ (100 MOI) alone (Figure 1b). By contrast, coinfection with AxdAdB-3 did not affect the X-gal staining of HeLa or WI-38 cells. Thus, addition of AxdAdB-3 effectively increased the CEA promoter-directed transgene expression in the GBC cells without increasing such expression in normal cells and, therefore, it enhanced the specificity of gene expression.

Next, we examined the CPE of the CEA promoter-directed HSVtk/GCV treatment with and without addition of different doses (0.1, 1 or 10 MOI) of AxdAdB-3. In the two lines of GBC cells, addition of AxdAdB-3 enhanced the CPE of AxCEAprTK (10 MOI)/GCV treatment in a dose-dependent manner (Figure 3a). Addition of AxdAdB-3 at 10 MOI, but not at 1 MOI, had a significant CPE even without the administration of GCV, suggesting that viral oncolysis became significant as the dose of AxdAdB-3 increased (Figure 3b). The CPE of the combination of AxCEAprTK (10 MOI)/GCV and AxdAdB-3 (1 MOI) was equivalent to that of the combination of AxCAHSVtk (10 MOI)/GCV and AxdAdB-3 (1 MOI) and it was greater than that of AxCAHSVtk (10 MOI)/GCV alone (Figure 4) or that

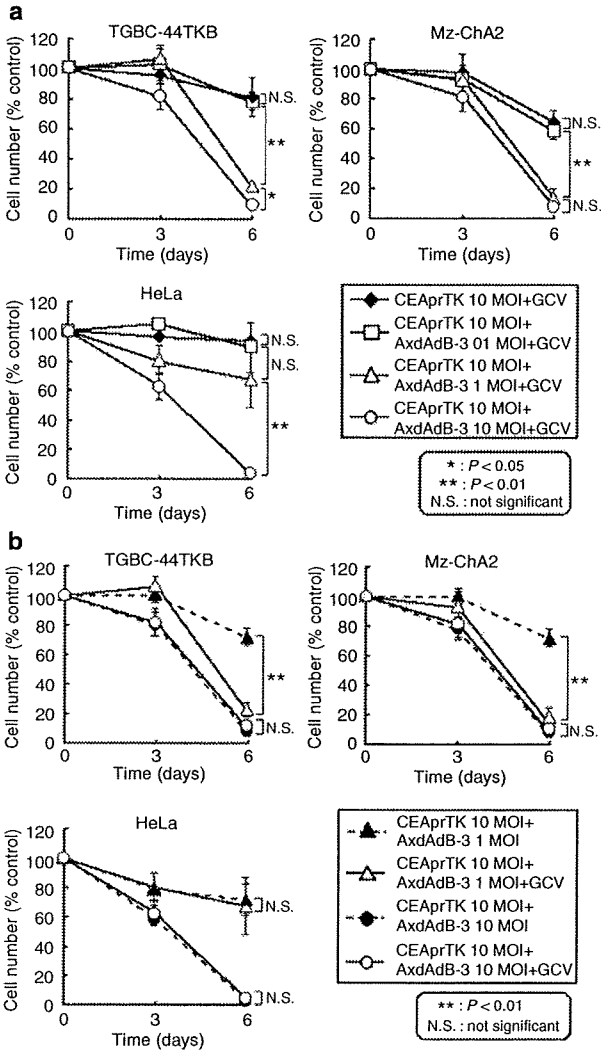

Figure 3 Effects of combination with AxdAdB-3 on the carcinoembryonic antigen (CEA) promoter-directed herpes simplex virus thymidine kinase (HSVtk)/ganciclovir (GCV) suicide gene treatment in gallbladder cancer (GBC), HeLa, and WI-38 cells. (**a**) Cells were infected with AxCEAprTK (10 multiplicity of infection, MOI) and AxdAdB-3 at 0, 0.1, 1 or 10 MOI, and were exposed to GCV ($20\,\mu g\,ml^{-1}$) 3 days later. The graphs show changes with time in numbers of viable cells (% control) as assessed by the WST-1 assay. The statistical significance of differences between the cytopathic effect (CPE) in the absence and in the presence of AxdAdB-3 at 0.1, 1 or 10 MOI is indicated by $^{**}P<0.01$, $^{*}P<0.05$ or NS (not significant). (**b**) Cells were infected with AxCEAprTK (10 MOI) and AxdAdB-3 at 1 or 10 MOI with and without administration of GCV ($20\,\mu g\,ml^{-1}$). Differences in the CPE with and without administration of GCV are indicated as significant $^{**}P<0.01$ or NS (not significant).

of a 10-fold higher dose of AxCEAprTK (100 MOI)/GCV (data not shown) in the two lines of GBC cells. In HeLa cells, coinfection with AxdAdB-3 had a dose-dependent CPE, whereas the combination of AxCEAprTK (10 MOI)/GCV and AxdAdB-3 (1 MOI) did not have a

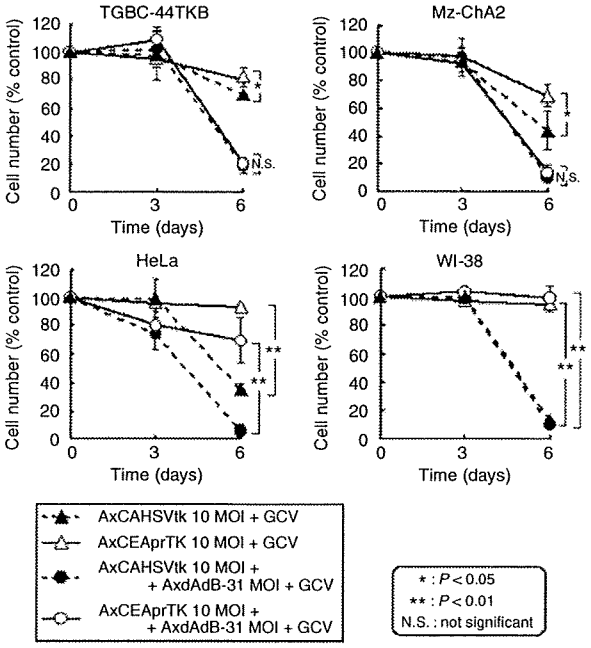

Figure 4 Effects of combination with AxdAdB-3 on the carcinoembryonic antigen (CEA) promoter-directed and nonspecific promoter-directed herpes simplex virus thymidine kinase (HSVtk)/ganciclovir (GCV) suicide gene treatment in gallbladder cancer (GBC), HeLa and WI-38 cells. Cells were infected with AxCEAprTK or AxCAHSVtk (10 multiplicity of infection, MOI) with and without AxdAdB-3 (1 MOI) and were exposed to GCV ($20\,\mu g\,ml^{-1}$) 3 days later. The graphs show changes in numbers of viable cells (% control) with time as determined by the WST-1. The significance of differences in the cytopathic effect (CPE) between AxCEAprTK/GCV and AxCAHSVtk/GCV is indicated by $^{**}P<0.01$, $^{*}P<0.05$ or NS (not significant).

potent CPE (Figure 3a), and this weak CPE was not enhanced by administration of GCV (Figure 3b). In normal WI-38 cells, the combination of AxCEAprTK (10 MOI)/GCV and AxdAdB-3 (1 MOI) did not have any CPE, whereas AxCAHSVtk (10 MOI)/GCV both with and without combination with AxdAdB-3 (1 MOI) had a marked CPE (Figure 4).

Quantitative assessment of the effects of combination with AxdAdB-3 on the CEA promoter-directed transgene expression in GBC, HeLa and WI-38 cells

In order to clarify the way in which the combination with AxdAdB-3 enhanced the CPE of AxCEAprTK/GCV on GBC cells, we evaluated quantitatively the CEA promoter-directed transgene (*LacZ*) expression from AxCEAprZ (100 MOI) by a β-galactosidase assay after coinfection of cells with AxdAdB-3 or with Ax1w1 as a control. Combination with AxdAdB-3 increased the β-galactosidase activity significantly at 10 MOI and increased further as the MOI was increased in the two lines of GBC cells (TGBC-44TKB and MzChA2) (Figure 5a). In particular, in TGBC-44TKB cells, the activity after coinfection with AxdAdB-3 (100 MOI) was approximately sevenfold higher than that without coinfection. By contrast, the combination did not increase the β-galactosidase activity

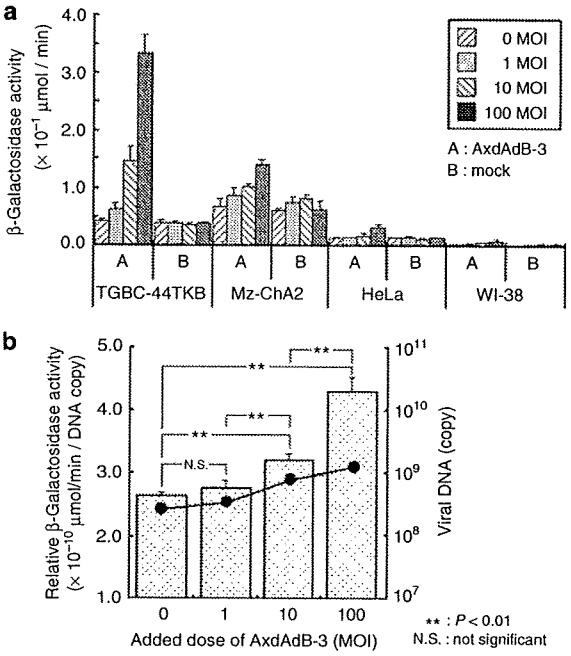

Figure 5 Quantitative assessment of the effects of combination with AxdAdB-3 on the carcinoembryonic antigen (CEA) promoter-directed β-galactosidase activity in gallbladder cancer (GBC) cells, HeLa and WI-38. (**a**) TGBC-44TKB, Mz-ChA2, HeLa and WI-38 cells were infected with AxCEAprZ (100 multiplicity of infection, MOI) and AxdAdB-3 or Ax1w1 at 0, 1, 10 or 100 MOI. At 10 h after the infection, β-galactosidase activity (μmol min^{-1}) in the cells was calculated from the absorbance at 420 nm. The results are shown as a histogram. (**b**) TGBC-44TKB cells were infected with AxCEAprZ (100 MOI) and AxdAdB-3 at 0, 1, 10 or 100 MOI. The β-galactosidase activity (μmol min^{-1}) and the number of copies of the AxCEAprZ viral genome were determined 10 h later. The number of copies of AxCEAprZ DNA is shown as a line. The ratio of β-galactosidase activity to the number of copies of AxCEAprZ DNA (μmol/min/DNA copy) is shown by columns. The statistical significance of differences among values is indicated by $^{**}P<0.01$ or NS (not significant).

in HeLa and WI-38 cells. Coinfection with Ax1w1, which is the same construct as AxdAdB-3 but lacks the *E1* region, did not affect the β-galactosidase activity in any of the cell lines tested.

To evaluate whether the increase in transgene expression upon combination with AxdAdB-3 was caused only by its activity as a helper virus that allowed the replication of AxCEAprZ, we examined the β-galactosidase activity and the number of copies of the AxCEAprZ genome simultaneously in TGBC-44TKB cells by quantitative PCR. Combination with AxdAdB-3 increased both the number of copies of AxCEAprZ genome (Figure 5b; dots connected by a line) and the β-galactosidase activity. We examined whether or not the combination had increased the activity of the CEA promoter of AxCEAprZ by calculating the relative β-galactosidase activity per copy of the AxCEAprZ genome (Figure 5b, columns). The relative β-galactosidase activity in TGBC-44TKB cells increased significantly upon combination with AxdAdB-3

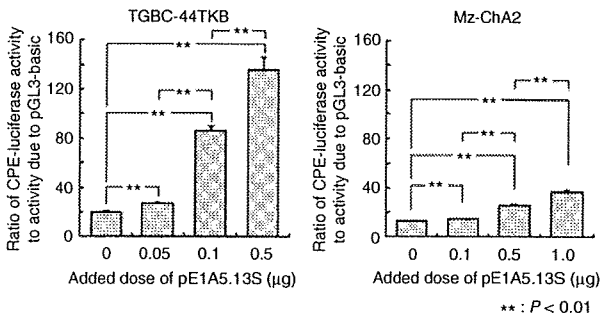

Figure 6 Effects of Ad E1A 13S on the activity of the carcinoembryonic antigen (CEA) promoter. We examined the direct effect of Ad E1A13S on the activity of the CEA promoter in plasmid co-transfection experiments. TGBC-44TKB and Mz-ChA2 cells were transfected with pE1A.13S at various concentrations in the presence of pGL3-CEApr. The CEA promoter-directed luciferase activity was evaluated in a dual luciferase assay. The ratio of CEA promoter-directed luciferase activity to the activity of luciferase due to pGL3-basic (control) is shown. The statistical significance of differences is indicated by $^{**}P<0.01$.

at 10 MOI and further elevated at 100 MOI (Figure 5b), suggesting that combination with AxdAdB-3 did, in fact, enhance the CEA promoter activity of AxCEAprZ.

Transactivation of CEA promoter activity by adenoviral E1A

To test our hypothesis that transactivation by E1A of AxdAdB-3 is responsible for the enhanced CEA promoter activity of AxCEAprZ, we examined the direct effect of adenoviral E1A13S on the activity of the CEA promoter in the plasmid co-transfection experiments. We co-transfected TGBC-44TKB and Mz-ChA2 cells with the pE1A5.13S at various concentrations in the presence of pGL3-CEApr. The luciferase activity directed by the CEA promoter relative to the activity due to pGL-3 basic was increased by the co-transfection with pE1A5.13S in a dose-dependent manner in both lines of GBC cells (Figure 6), and in particular in TGBC-44TKB cells. These results proved that adenoviral E1A13S can transactivate the CEA promoter activity.

Effects of the combination therapy with AxdAdB-3 and AxCEAprTK/GCV in normal cells

In order to further examine the safety of the combined use of AxdAdB-3 and AxCEAprTK, we infected normal WI-38 cells and primary epithelial cells with AxCEAprTK and AxdAdB-3 at different dose ratio (1:10, 1:1, 10:1) with a fixed high total viral dose of 220 MOI, with and without subsequent administration of GCV (Figure 7). Even with this high total viral dose, the combination of AxdAdB-3 (20 MOI) and AxCEAprTK (200 MOI) had no CPE on WI-38 cells and only a mild CPE on epithelial cells, suggesting the safety of this combination. When the relative dose of AxdAdB-3 was increased to the same as or greater than the dose of AxCEAprTK, some CPE was evident in both normal cells, even in the absence of GCV

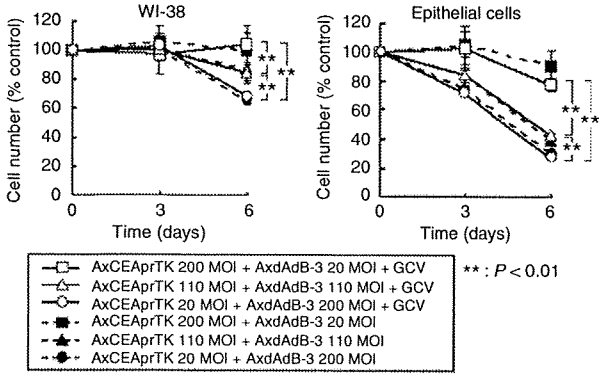

Figure 7 Cytopathic effects of AxdAdB-3 and the carcinoembryonic antigen (CEA) promoter-directed herpes simplex virus thymidine kinase (HSVtk) suicide gene vector with and without administration of ganciclovir (GCV) in normal cells (WI-38 cells and a primary culture of epithelial cells). In order to examine the safety of the combined use of AxdAdB-3 and AxCEAprTK, we infected normal WI-38 cells and epithelial cells with AxCEAprTK and AxdAdB-3 at different dose ratios (10:1, 1:1 or 1:10) with a fixed total viral dose (220 multiplicity of infection, MOI) with and without administration of GCV (20 $\mu g\,ml^{-1}$). Changes are shown in the numbers of viable cells (% control) as assessed by the WST-1 assay. The statistical significance of differences in values between groups treated with GCV are indicated as $^{**}P<0.01$.

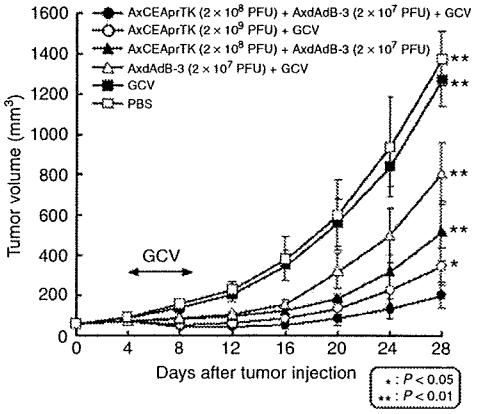

Figure 8 Antitumor effects of the intratumorally (i.t.) injected combination of AxdAdB-3 and carcinoembryonic antigen (CEA) promoter-directed herpes simplex virus thymidine kinase (HSVtk)/ganciclovir (GCV) therapy on subcutaneously implanted gallbladder cancer (GBC) in severe combined immunodeficiency disease (SCID) mice. TGBC-44TKB cells (1×10^7 cells per 100 µl) were subcutaneously (s.c.) injected into the left flank of mice and tumors were allowed to grow to 5–6 mm in diameter. Then, mice were randomly separated into six groups ($n=6$ in each group) as indicated. Viruses were injected i.t. on day 1 and intraperitoneally (i.p.) ganciclovir (GCV) (200 $mg\,kg^{-1}$) was given daily from days 4 to 9. The tumor volume was periodically determined as described in the text. The statistical significance of differences in tumor volumes, compared with tumors treated with AxdAdB-3 (2×10^7 PFU) plus AxCEAprTK (2×10^8 PFU)/GCV, are indicated by $^{**}P<0.01$ or $^{*}P<0.05$.

(Figure 7), because of the high total viral dose (220 MOI) applied.

Efficacy in vivo *of the combination therapy with AxdAdB-3 and AxCEAprTK/GCV in SCID mice with subcutaneously implanted GBC*

Finally, we evaluated the antitumor effects *in vivo* of the combined use of AxdAdB-3 and CEA promoter-directed suicide gene therapy in SCID mice with subcutaneously implanted GBC (Figure 8). The dose of AxCEAprTK (2×10^8 PFU) in the combination was reduced to one-tenth of the dose used for the conventional suicide gene therapy with AxCEAprTK (2×10^9 PFU) alone, and a further reduced dose of AxdAdB-3 (2×10^7 PFU) was used in the combination. AxCEAprTK (2×10^9 PFU)/GCV therapy and the combination therapy of AxdAdB-3 (2×10^7 PFU) plus AxCEAprTK (2×10^8 PFU)/GCV both reduced the tumor volume, measured on day 5 through 8, when GCV was administered, and tumor growth was suppressed significantly ($P<0.01$) more than after administration of low-dose AxdAdB-3 (2×10^7 PFU), PBS, or GCV alone. Furthermore, the combination of AxdAdB-3 (2×10^7 PFU) plus AxCEAprTK (2×10^8 PFU)/GCV suppressed tumor growth significantly ($P<0.05$) more effectively than AxCEAprTK (2×10^9 PFU)/GCV, the conventional suicide gene therapy using high-dose replication-defective vector.

Discussion

The development of effective combination therapy with replicative oncolytic virus is a recent topic in cancer gene therapy.[12,13,24] All previous studies which examined the combination of CRAd and suicide gene therapy have used single 'armed' CRAd, in which the CRAd was armed with a suicide gene.[25–33] Only few studies have examined the two-vector systems, which included a complementary vector system for replication[42] or combinations of CRAds with replication-deficient Ads expressing cytokine genes[43,44] or a dominant-negative insulin-like growth factor gene.[45] To our knowledge, our study is the first to examine the two-vector combination of a CRAd and a replication-deficient Ad carrying a suicide gene (*HSVtk*) with or without a tumor-specific promoter.

Using AxdAdB3, an E1A, E1B double-restricted CRAd in combination with the GDEPT with HSVtk/GCV directed by CEA promoter, we developed a potentially effective and safe combination therapy for CEA producing malignancies, such as GBC. The merits of this approach can be summarized as follows. First, a low helper dose of the CRAd allowed tumor-specific proliferation of the replication-defective vector that carries the CEA promoter-directed *HSVtk* gene. Second, the coinfection with the CRAd enhanced the low potency of the CEA promoter, presumably through the transactivation function of the Ad E1A, and thus enhanced still further the tumor-specific expression of the *HSVtk* gene and its antitumor effects. Third, the use of CRAd allowed the reduction of dose of the *HSVtk* vector and thus can expect a greater margin of safety with

respect to acute systemic inflammatory reaction caused by the vectors.

The therapeutic efficacy of conventional suicide gene therapy using CEA promoter was limited due to the low potency of the promoter as compared with nonspecific promoters. Indeed, the CPEs of AxCEAprTK/GCV treatment on the two lines of GBC cells *in vitro* were significantly weaker than those of AxCAprTK/GCV, a HSVtk/GCV treatment in which expression of *HSVtk* was regulated by a nonspecific CAG promoter (Figure 2). Previous efforts to overcome the low potency of the CEA promoter included insertion of a Cre/lox P system,[9] a CEA promoter-enhancer system,[10] or a GAL4 gene-regulatory system[11] in the vector. However, these modifications failed to overcome the limitations of gene delivery to the tumor cells, which have become uniformly evident in gene therapy trials using replication-defective vectors.

Addition of AxdAdB-3, even at a low dose, greatly increased the level and the extent of transgene expression from the replication-defective AxCEAprZ vector (Figure 1; Figure 5a). This effect was due in part to the function of the CRAd as a helper virus as described previously,[17,43–45] providing the replication-defective AxCEAprZ vector with E1 proteins, which allowed its replication (Figure 5b). In addition, we found that the CRAd also significantly increased the activity of the CEA promoter per individual copy of the AxCEAprZ genome (Figure 5b). We proved that adenoviral E1A13S protein can transactivate the CEA promoter, as the co-transfected pE1A5.13S enhanced the CEA promoter-directed luciferase activity of pGL3-CEApr (Figure 6). Adenoviral E1A13S can function as a transcriptional activator to stimulate transcription from a variety of promoters upon association with various transcription factors, such as ATF-2, Sp1 and USF[46] and components of the basal transcription-initiation complex.[47] Hauck and Stanners[48] reported that USF and Sp1 bound to the regulatory elements of the CEA promoter and that USF controlled the transcription of CEA. Therefore, it is assumed that transactivaton of the CEA promoter by Ad E1A13S is mediated by USF and/or Sp1.

Addition of AxdAdB-3 even at a low dose (1 MOI) resulted in a marked enhancement of the *in vitro* antitumor effects of AxCEAprTK (10 MOI)/GCV therapy on GBC cells with strong CEA-promoter activity (Figure 3). This combination was even more potent than high-dose (100 MOI) AxCEAprTK/GCV alone (data not shown). This was confirmed *in vivo* when the combination demonstrated higher antitumor effects than the conventional suicide gene therapy using replication-defective AxCEAprTK at high dose followed by GCV administration (Figure 8). In this case, the suicide gene was the major player and the CRAd played a role as the supporting cast. When the dose of the CRAd was increased, the anititumor effects became evident even without the administration of GCV (Figure 3), suggesting that the oncolytic effects of the CRAd had become the major factor whereas the suicide gene played a minor role. The latter results suggest that the relative contribution of viral oncolysis and suicide gene effects can be altered by changing the relative doses of the two vectors. Future studies should test this efficacy of changing the dose ratio of the two vectors *in vivo*, for their possible tailored use.

When CRAds are used in combination with additional cytotoxic genes to enhance the antitumor effects, the safety of the individual CRAds and the additional therapeutic vector would be critical. Therefore, we used AxdAdB-3, a CRAd that showed an increased safety profile to several normal cells *in vitro* than ONYX-015-type E1B 55 kDa defective CRAd in our previous study.[22] The safety of ONYX-015 has been proved in many clinical studies.[14,15,20] We also used AxCEAprTK, a nonreplicative Ad in which the genes for HSVtk was driven by a tumor-specific promoter to maximize the safety of the combination therapy. Indeed, the combination of AxCEAprTK/GCV and AxdAdB-3 was less toxic to normal WI-38 cells than AxCAHSVtk/GCV alone or its combination with AxdAdB-3 (Figure 4). However, as *in vitro* cells in culture are not in G1 arrested state, CRAds, including AxdAdB-3, can replicate to some extent and cause some cytopathy especially when large dose of the virus is applied. Only relative safety between vectors, but not absolute safety of vectors can be assessed by *in vitro* experiments. Indeed, ONYX-015, of which safety has been proved clinically, has been shown in several reports to cause significant cytopathy in normal cells *in vitro*.[20,21] Even with this experimental restraints, when a large total dose (220 MOI) of viral combination was applied to normal cells, the combination of AxdAdB-3 (20 MOI) plus AxCEAprTK (200 MOI) with GCV administration exhibited no toxicity, whereas the combination of AxdAdB-3 (200 MOI) plus AxCEAprTK (20 MOI) without CCV administration showed significant cytopathy, in normal cells (Figure 7). This suggests the relative safety of the former combination, but does not necessary suggest the risk of the latter combination from the above reason and from the fact that only 11 MOI (1 of 20 of the dose that used for normal cells) was required to kill cancer cells by these combinations. To assess the true safety, these *in vitro* data need to be confirmed by future *in vivo* experiments using a Syrian hamster model, a recently found permissive animal model for Ad.[49]

Studies using multivector systems have been limited, but deserve more attention and testing from the following reasons. First, the results of the CRAds armed with suicide genes have been conflicting.[25–33] Although several reports have indicated that the HSVtk/GCV system provides additive anticancer effects to oncolytic virus,[25–29] others suggest that they give no supplemental effect or they might even do harm by eradicating the viruses.[30–33] Especially, Wildner and Morris[31] have demonstrated that the addition of HSVtk/GCV system did not play any role in the face of very robust virus, whereas it provided the CRAd that had lost some replication efficacy and oncolytic activity with additional antitumor effects. The use of two-vector systems can avoid the potentially negative effects of arming the therapeutic genes that can reduce the replicating and

oncolytic efficacy of the CRAd. Second, two vectors can accommodate larger or multiple genes that a single vector cannot. Third, the overall anticancer effects of the combination of viral oncolysis and suicide gene effects seem to be complex and probably depend on multiple factors of the cancer (susceptibility to the viral infection, oncolysis and suicide gene products), the virus (potential for replication and oncolysis), the suicide gene (potency and its bystander effects)[14] and the prodrug (timing of administration).[28,33] Thus, it would be better if the combination therapy can be tailored for different types of cancers and patients. Indeed, in our previous study of a CRAd armed with a suicide gene, uracil phosphoribosyltransferase (UPRT), followed by administration of its prodrug, 5-fluorouracil (5-FU), we found additional antitumor effects on biliary cancers only when the timing of 5-FU administration was properly chosen depending on the Ad infectivity of the cancers.[33] In the armed one-vector system, this timing of the prodrug administration is the only factor that clinicians can possibly modify to maximize the efficacy. By contrast, the two-vector system may also allow clinicians to tailor the suicide gene effects and viral oncolytic effects by changing the relative doses of the two vectors, as discussed above, depending on the nature of the target cancer: whether it is more susceptible to suicide gene/prodrug effect or rather to viral oncolytic effect. Thus, the combination therapy would at least be complimentary. In addition, the combination would give synergistic effects in some case when the CRAd enhanced the activity of tumor-specific promoter and thus the expression of transgene. Taken together, as cancer chemotherapy progressed from the era of monotherapy to today's multidrug regimens, combination virotherapy may offer great promise and flexibility in future attempts at cancer gene therapy. Further extensive studies are necessary to characterize the interactions among multiple vectors and to establish their tailored use for the treatment of a variety of cancers.

One might assume that the types of cancer responsive to the combination therapy is limited as the replication of AxdAdB-3 requires abnormalities in both the pRb and p53 pathways, whereas the expression of AxCEAprTK requires active CEA promoter. However, abnormalities in p53 or its upstream signals (p14, mdm2 and ATM), as well as those in the components of the pRb signaling pathway (pRb, p16, CDK2 and CDK4/6), are likely to be found in nearly all cancer cells.[50] Approximately 80% of patients with GBC have some abnormalities in p16 and more than 50% of the patients have mutations in p53.[35–39] In addition, the activity of the CEA promoter is elevated in many gastrointestinal cancers including GBC.[39] Therefore, it seems reasonable to anticipate efficacy of the combination therapy in many patients with GBC or other CEA-producing malignancies.

Abbreviations

Ad, adenovirus; CAG, chicken β-actin enhancer β-globin promoter; CEA, carcinoembryonic antigen; CPE, cytopathic effect; CRAd, conditionally replicative adenovirus; 5-FU, 5-fluorouracil; GB, gallbladder; GBC, gallbladder cancer; GCV, ganciclovir; HSVtk, herpes simplex virus thymidine kinase gene; i.p., intraperitoneally; i.t., intratumorally; MOI, multiplicity of infection; pRb, retinoblastoma protein; PFU, plaque-forming unit(s); s.c., subcutaneously; SCID, severe combined immunodeficiency disease; SV40, senminum virus 40.

Acknowledgements

Dr Abei and Dr Yokoyama are supported by Grants-In-Aid from the Ministry of Education, Culture, Sports, Science and Technology of Japan.

References

1 Misra S, Chaturvedi A, Misra NC, Sharma ID. Carcinoma of the gallbladder. *Lancet Oncol* 2003; **4**: 167–176.
2 Donohue JH, Stewart AK, Menck HR. The national cancer data base report on carcinoma of the gallbladder, 1989–1995. *Cancer* 1998; **83**: 2618–2628.
3 Osaki T, Tanio Y, Tachibana I, Hosoe S, Kumagai T, Kawase I *et al*. Gene therapy for carcinoembryonic antigen-producing human lung cancer cells by cell type-specific expression of herpes simplex virus thymidine kinase gene. *Cancer Res* 1994; **54**: 5258–5261.
4 Tanaka T, Kanai F, Okabe S, Yoshida Y, Wakimoto H, Hamada H *et al*. Adenovirus-mediated prodrug gene therapy for carcinoembryonic antigen-producing human gastric carcinoma cells *in vitro*. *Cancer Res* 1996; **56**: 1341–1345.
5 Tanaka T, Kanai F, Lan K-H, Ohashi M, Shiratori Y, Yoshida Y *et al*. Adenovirus-mediated gene therapy of gastric carcinoma using cancer-specific gene expression *in vivo*. *Biochem Biophys Res Commun* 1997; **231**: 775–779.
6 Brand K, Loser P, Arnold W, Bartels T, Strauss M. Tumor cell-specific transgene expression prevents liver toxicity of the adeno-HSVtk/GCV approach. *Gene Ther* 1998; **5**: 1363–1371.
7 Kaneko S, Hallenbeck P, Kotani T, Nakabayashi H, McGarrity G, Tamaoki T *et al*. Adenovirus-mediated gene therapy of hepatocellular carcinoma using cancer-specific gene expression. *Cancer Res* 1995; **55**: 5283–5287.
8 Hammarstrom S. The carcinoembryonic antigen (CEA) family: structures, suggested functions and expression in normal and malignant tissues. *Semin Cancer Biol* 1999; **9**: 67–81.
9 Kijima T, Osaki T, Nishino K, Kumagai T, Funakoshi T, Goto H *et al*. Application of the Cre recombinase/*lox P* system further enhances antitumor effects in cell type-specific gene therapy against carcinoembryonic antigen-producing cancer. *Cancer Res* 1999; **59**: 4906–4911.
10 Nyati MK, Sreekumar A, Li S, Zhang M, Rynkiewicz SD, Chinnaiyan AM *et al*. High and selective expression of yeast cytosine deaminase under a carcinoembryonic antigen promoter-enhancer. *Cancer Res* 2002; **62**: 2337–2342.
11 Koch PE, Guo ZS, Kagawa S, Gu J, Roth JA, Fang B. Augmented transgene expression from carcinoembryonic antigen (CEA) promoter via a GAL4 gene-regulatory system. *Mol Ther* 2001; **3**: 278–283.
12 Chiocca EA. Oncolytic viruses. *Nat Rev* 2002; **2**: 938–950.

13 Everts B, van der Poel HG. Replication-selective oncolytic viruses in the treatment of cancer. *Cancer Gene Ther* 2005; **12**: 141–161.
14 Ries S, Korn WM. ONYX-015: mechanism of action and clinical potential of a replication-selective adenovirus. *Br J Cancer* 2002; **86**: 5–11.
15 Khuri FR, Nemunaitis J, Ganly I, Arseneau J, Tannock IF, Romel L *et al.* A controlled trial of intratumoral ONYX-015, a selectively replicating adenovirus, in combination with cisplatin and 5-fluorouracil in patients with recurrent head and neck cancer. *Nat Med* 2000; **6**: 879–885.
16 Heise C, Hermiston T, Johnson L, Brooks G, Jhoannes AS, Williams A *et al.* An adenovirus E1A mutant that demonstrates potent and selective systemic anti-tumoral efficacy. *Nat Med* 2000; **6**: 1134–1139.
17 Doronin S, Toth K, Kuppuswamy M, Ward P, Tollefson AE, Wold WSM. Tumor-specific, replication-competent adenovirus vectors overexpressing the adenovirus death protein. *J Virol* 2000; **74**: 6147–6155.
18 Rothmann T, Hengstermann A, Whitaker NJ, Scheffner M, Hausen H. Replication of ONYX-015, a potential anticancer adenovirus, is independent of p53 status in tumor cells. *J Virol* 1998; **72**: 9470–9478.
19 Harada JN, Berk AJ. p53-Independent and -dependent requirements for E1B-55K in adenovirus type 5 replication. *J Virol* 1999; **73**: 5333–5344.
20 Makower D, Rozenblit A, Kaufman H, Edelman M, Lane ME, Zwiebel J *et al.* Phase II clinical trial of intralesional administration of the oncolytic adenovirus ONYX-015 in patients with hepatobiliary tumors with correlative p53 studies. *Clin Cancer Res* 2003; **9**: 693–702.
21 Wadler S, Yu B, Tan J-Y, Kaleya R, Rozenblit A, Makower D *et al.* Persistent replication of the modified chimeric adenovirus ONYX-015 in both tumor and stromal cells from a patient with gallbladder carcinoma implants. *Clin Cancer Res* 2003; **9**: 33–43.
22 Fukuda K, Abei M, Ugai H, Seo E, Wakayama M, Murata T *et al.* E1A, E1B double-restricted oncolytic adenovirusfor gene therapy of gallbladder cancer. *Cancer Res* 2003; **63**: 4434–4440.
23 Gomez-Manzano C, Balague C, Alemany R, Lemoine MG, Mitlianga P, Jiang H *et al.* A novel E1A-E1B mutant adenovirus induces glioma regression *in vivo*. *Oncogene* 2004; **23**: 1821–1828.
24 Chu RL, Post DE, Khuri FR, Van Meir EG. Use of replicating oncolytic adenoviruses in combination therapy for cancer. *Clin Cancer Res* 2004; **10**: 5299–5312.
25 Freytag SO, Rogulski KR, Paielli DL, Gilbert JD, Kim JH. A novel three-pronged approach to kill cancer cells selectively: concomitant viral, double-suicide gene, and radiotherapy. *Human Gene Ther* 1998; **9**: 1323–1333.
26 Rogulski KR, Wing MS, Paielli DL, Gilbert JD, Kim JH, Freytag SO. Double suicide gene therapy augments the antitumor activity of a replication-competent lytic adenovirus through enhanced cytotoxicity and radiosensitization. *Human Gene Ther* 2000; **11**: 67–76.
27 Wildner O, Blaese RM, Morris JC. Therapy of colon cancer with oncolytic adenovirus is enhanced by the addition of herpes simplex virus-*thymidine kinase*. *Cancer Res* 1999; **59**: 410–413.
28 Wildner O, Morris JC, Vahanian NN, Ford Jr H, Ramsey WJ, Blaese RM. Adenoviral vectors capable of replication improve the efficacy of HSVtk/GCV suicide gene therapy of cancer. *Gene Ther* 1999; **6**: 57–62.
29 Nanda D, Vogels R, Havenga H, Azezaat CJ, Bout A, Smit PS. Treatment of malignant gliomas with a replicating adenoviral vector expressing herpes simplex virus-thymidine kinase. *Cancer Res* 2001; **61**: 8743–8750.
30 Morris JC, Wildner O. Therapy of head and neck squamous cell carcinoma with an oncolytic adenovirus expressing HSV-tk. *Mol Ther* 2000; **1**: 56–62.
31 Wildner O, Morris JC. The role of the E1B 55kDa gene product in oncolytic adenoviral vectors expressing herpes simplex virus-tk: assessment of antitumor efficacy and toxicity. *Cancer Res* 2000; **60**: 4167–4174.
32 Lambright ES, Amin K, Wiewrodt R, Force SD, Lanuti M, Propert KJ, *et al.* Inclusion of the herpes simplex thymidine kinase gene in a replicating adenovirus does not augment antitumor efficacy. *Gene Ther* 2001; **8**: 946–953.
33 Seo E, Abei M, Wakayama M, Fukuda K, Ugai H, Murata T *et al.* Effective gene therapy for biliary tract cancer by a conditionally replicative adenovirus carrying uracil phosphoribosyltransferase (UPRT) gene: Significance of timing of 5-fluorouracil administration. *Cancer Res* 2005; **65**: 546–552.
34 Kamel D, Paakko P, Nuorva K, Vahakangas K, Soini Y. p53 and c-erbB-2 protein expression in adenocarcinomas and epithelial dysplasias of the gallbladder. *J Pathol* 1993; **170**: 67–72.
35 Hanada K, Itoh M, Fujii K, Tsuchida A, Ooishi H, Kajiyama G. K-ras and p53 mutations in stage I gallbladder carcinoma with an anomalous junction of the pancreaticobiliary duct. *Cancer* 1996; **77**: 452–458.
36 Caca K, Feisthammel J, Klee K, Tannapeel A, Witzigmann H, Wittekind C *et al.* Inactivation of the INK4A/ARF locus and p53 in sporadic extrahepatic bile duct cancers and bile tract cancer cell lines. *Int J Cancer* 2002; **97**: 481–488.
37 Yoshida S, Todoroki T, Ichikawa Y, Hanai S, Suzuki H, Hori M *et al.* Mutations of *p16*Ink4/*CDKN2* and *p15*Ink4B/*MTS2* gene in biliary tract cancers. *Cancer Res* 1995; **55**: 2756–2760.
38 Shi YZ, Hui AM, Li X, Takayama T, Makuuchi M. Overexpression of retinoblastoma protein predicts decreased survival and correlates with loss of p16INK4 protein in gallbladder carcinomas. *Clin Cancer Res* 2000; **6**: 4096–4100.
39 Maxwell P, Davis RI, Sloan J. Carcinoembryonic antigen (CEA) in benign and malignant epithelium of the gallbladder, extrahepatic bile ducts, and ampulla of Vater. *J Pathol* 1993; **170**: 73–76.
40 Shinoura N, Yoshida Y, Tsunoda R, Ohashi M, Zhang W, Asai A *et al.* Highly augmented cytopathic effect of a fiber-mutant E1B-defective adenovirus for gene therapy of gliomas. *Cancer Res* 1999; **59**: 3411–3416.
41 Katho S, Ozawa K, Kondoh S, Soeda E, Israel A, Shiroki K *et al.* Identification of sequences responsible for positive and negative regulation by E1A in the promoter of H-2K^{bml} class I MHC gene. *EMBO J* 1990; **9**: 127–135.
42 Alemany R, Lai S, Lou Y-C, Jan H-Y, Fang X, Zhang W-W. Complementary adenoviral vectors for oncolysis. *Cancer Gene Ther* 1999; **6**: 21–25.
43 Motoi F, Sunamura M, Ding L, Duda DG, Yoshida Y, Zhang W *et al.* Effective gene therapy for pancreatic cancer by cytokines mediated by restricted replication-competent adenovirus. *Hum Gene Ther* 2000; **11**: 223–235.
44 Nagayama Y, Nakao K, Hayakawa T, Niwa M. Enhanced antitumor effect of combined replicative adenovirus and non-replicative adenovirus expressing interleukin-12 in an immunocompetent mouse model. *Gene Ther* 2003; **10**: 1400–1403.

45 Lee C-T, Park K-H, Yanagisawa K, Adachi Y, Ohm JF, Nadaf S *et al.* Combination therapy with conditionally replicative adenovirus and replication defective adenovirus. *Cancer Res* 2004; **64**: 6660–6665.
46 Liu F, Green MR. Promoter targeting by adenovirus E1A through interaction with different cellular DNA-binding domains. *Nature* 1994; **368**: 520–525.
47 Flint J, Shenk T. Viral transactivating proteins. *Annu Rev Genet* 1997; **31**: 177–212.
48 Hauck W, Stanners CP. Transcriptional regulation of the carcinoembryonic antigen gene. *J Biol Chem* 1995; **8**: 3602–3610.
49 Thomas MA, Spencer JF, La Regina MC, Dhar D, Tollefson AE, Toth K *et al.* Syrian hamster as a permissive immunocompetent animal model for the study of oncolytic adenovirus vectors. *Cancer Res* 2006; **66**: 1270–1276.
50 Sherr CJ, McCormick F. The Rb and p53 pathways in cancer. *Cancer Cell* 2002; **2**: 103–112.

THE JOURNAL OF BIOLOGICAL CHEMISTRY VOL. 284, NO. 38, pp. 25585–25592, September 18, 2009

Translesional DNA Synthesis through a C8-Guanyl Adduct of 2-Amino-1-methyl-6-phenylimidazo[4,5-*b*]pyridine (PhIP) *in Vitro*

REV1 INSERTS dC OPPOSITE THE LESION, AND DNA POLYMERASE κ POTENTIALLY CATALYZES EXTENSION REACTION FROM THE 3′-dC TERMINUS[*][S]

Received for publication, June 25, 2009, and in revised form, July 16, 2009 Published, JBC Papers in Press, July 23, 2009, DOI 10.1074/jbc.M109.037259

Hirokazu Fukuda[‡], Takeji Takamura-Enya[§], Yuji Masuda[¶], Takehiko Nohmi[‖], Chiho Seki[‡], Kenji Kamiya[¶], Takashi Sugimura[‡], Chikahide Masutani[**], Fumio Hanaoka[1], and Hitoshi Nakagama[‡2]**

From the [‡]Biochemistry Division, National Cancer Center Research Institute, 1-1, Tsukiji 5, Chuo-ku, Tokyo 104-0045, the [§]Department of Applied Chemistry, Faculty of Engineering, Kanagawa Institute of Technology, Ogino 1030, Atsugi, Kanagawa 243-0292, the [¶]Department of Experimental Oncology, Research Institute for Radiation Biology and Medicine, Hiroshima University, Kasumi 1-2-3, Minami-ku, Hiroshima, Hiroshima 734-8553, the [‖]Division of Genetics and Mutagenesis, National Institute of Health Sciences, Kamiyoga 1-18-1, Setagaya-ku, Tokyo 158-8501, and the [**]Cellular Biology Laboratory, Graduate School of Frontier Biosciences, Osaka University, Yamada-oka 1-3, Suita, Osaka 565-0871, Japan

2-Amino-1-methyl-6-phenylimidazo[4,5-*b*]pyridine (PhIP) is the most abundant heterocyclic amine in cooked foods, and is both mutagenic and carcinogenic. It has been suspected that the carcinogenicity of PhIP is derived from its ability to form DNA adducts, principally dG-C8-PhIP. To shed further light on the molecular mechanisms underlying the induction of mutations by PhIP, *in vitro* DNA synthesis analyses were carried out using a dG-C8-PhIP-modified oligonucleotide template. In this template, the dG-C8-PhIP adduct was introduced into the second G of the TCC GGG AAC sequence located in the 5′ region. This represents one of the mutation hot spots in the rat *Apc* gene that is targeted by PhIP. Guanine deletions at this site in the *Apc* gene have been found to be preferentially induced by PhIP in rat colon tumors. DNA synthesis with A- or B-family DNA polymerases, such as *Escherichia coli* polymerase (pol) I and human pol δ, was completely blocked at the adducted guanine base. Translesional synthesis polymerases of the Y-family, pol η, pol ι, pol κ, and REV1, were also used for *in vitro* DNA synthesis analyses with the same templates. REV1, pol η, and pol κ were able to insert dCTP opposite dG-C8-PhIP, although the efficiencies for pol η and pol κ were low. pol κ was also able to catalyze the extension reaction from the dC opposite dG-C8-PhIP, during which it often skipped over one dG of the triple dG sequence on the template. This slippage probably leads to the single dG base deletion in colon tumors.

Heterocyclic amines (HCAs)[3] are naturally occurring genotoxic carcinogens produced from cooking meat (1). The initial carcinogenic event induced by HCAs is metabolic activation and subsequent covalent bond formation with DNA (1, 2). 2-Amino-1-methyl-6-phenylimidazo[4,5-*b*]pyridine (PhIP) is the most abundant heterocyclic amine in cooked foods, and was isolated from fried ground beef (3, 4). PhIP possesses both mutagenic and carcinogenic properties (5–8). Epidemiological studies have revealed that a positive correlation exists between PhIP exposure and mammary cancer incidence (9). PhIP induces colon and prostate cancers in male rats and breast cancer in female rats (8, 10).

The incidences of colon, prostate, and breast cancers are steadily increasing in Japan and other countries and this has been found to correlate with a more Westernized lifestyle. Elucidating the molecular mechanisms underlying PhIP-induced mutations is therefore of considerable interest. It is suspected that the carcinogenicity of PhIP is derived from the formation of DNA adducts, principally dG-C8-PhIP (11–14) (see Fig. 1). Studies of the mutation spectrum of PhIP in mammalian cultured cells and transgenic animals have revealed that G to T transversions are predominant and that guanine deletions from G stretches, especially from the 5′-GGGA-3′ sequence, are significant (15–20). Five mutations in the *Apc* gene were detected in four of eight PhIP-induced rat colon tumors, and all of these mutations involved a single base deletion of guanine from 5′-GGGA-3′ (21). These mutation spectra are thought to be influenced by various factors, including the primary structure of the target gene itself, the capacity of translesional DNA polymerases, and the activity level of repair enzymes (1). However, the molecular mechanisms underlying the formation of PhIP-induced mutations are largely unknown.

To shed further light on the molecular processes that underpin the mutations induced by PhIP, we performed *in vitro* DNA synthesis analyses using a dG-C8-PhIP-modified oligonucleotide template. We have recently reported the successful synthesis of oligonucleotides harboring a site-specific PhIP adduct

* This work was supported by Kakenhi Grant 19570144.
[S] The on-line version of this article (available at http://www.jbc.org) contains supplemental Table S1 and Figs. S1–S6.
[1] Present address: Dept. of Life Science, Faculty of Science, Gakushuin University, Mejiro 1-5-1, Toshima-ku, Tokyo 171-8588, Japan.
[2] To whom correspondence should be addressed. Tel.: 81-3-3542-2511; Fax: 81-33542-2530; E-mail: hnakagam@ncc.go.jp.
[3] The abbreviations used are: HCA, heterocyclic amines; PhIP, 2-amino-1-methyl-6-phenylimidazo[4,5-*b*]pyridine; TLS, translesional DNA synthesis; IQ, 2-amino-3-methylimidazo[4,5-*f*]quinoline; pol, DNA polymerase; DTT, dithiothreitol; PCNA, proliferating cell nuclear antigen; PIPES, 1,4-piperazinediethanesulfonic acid.

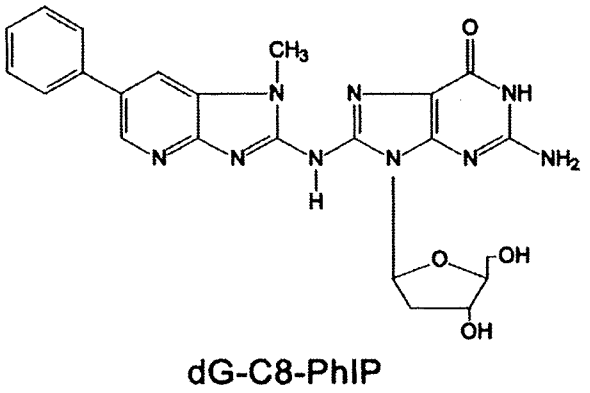

dG-C8-PhIP

FIGURE 1. **Structure of the dG-C8-PhIP adduct.**

(22). In our current study, we used this synthesis method to construct a 32-mer oligonucleotide template containing a 5′-TTCGGGAAC-3′ sequence with different site-specific PhIP adducts. We then utilized the resulting constructs in DNA synthesis analyses to reconstitute the PhIP-induced mutagenesis of the rat *APC* gene. DNA synthesis reactions with A- or B-family DNA polymerases, such as *Escherichia coli* pol I and human pol δ, or translesional synthesis (TLS) polymerases of the Y-family, pol η, pol ι, pol κ, and REV1, were carried out. Kinetic analyses of pol κ and REV1, for which TLS activities at the PhIP adduct were detected, were also performed.

EXPERIMENTAL PROCEDURES

Enzymes and Materials—T4 polynucleotide kinase and T4 DNA ligase were purchased from Toyobo Biochem (Osaka, Japan) and Takara Biotech (Tokyo Japan), respectively. Other materials were obtained from Sigma or Wako (Osaka, Japan).

DNA Polymerases and PCNA—Human recombinant DNA polymerases, pol δ, pol η, pol κ, and REV1, and PCNA were expressed and purified as described previously (23–27). Human DNA polymerase α and DNA polymerase ι were purchased from Chimerx. *E. coli* DNA polymerases I (Takara Biotech) and Klenow Fragment (Takara Biotech), and thermophilic bacterial DNA polymerases, r*Taq* (Toyobo Biochem) and *Tth* (Toyobo Biochem) were used.

Oligonucleotides—The method used to chemically synthesize three 9-mer oligonucleotides, 5′-TCCGGGAAC-3′, containing a PhIP adduct on either the first, second, or third G (p9B, p9C, and p9D, respectively) has been described previously (22). All other synthetic oligonucleotides were synthesized and purified using a reverse-phase cartridge (Operon Biotech Japan (Tokyo, Japan). The 23-mer oligonucleotides: p23a, 5′-TGACTCGTCGTGACTGGGAAAAC-3′, and p23b, 5′-GTCACGACGAGTCAGTTCCCGGA-3′, were used for constructing the template oligonucleotides as described below. A 32-mer oligonucleotide without the PhIP adduct, p32A, was used as a control template (see Table 1). Its 3′ complementary 29-, 28-, 27-, 26-, 22-, and 17-mer sequences (p29, p28, p27, p26, p22, and p17) were used as extension primers (see Table 1).

Construction of Template-Primer Complexes Containing the PhIP Adduct—A 32-mer template oligonucleotide p32C (see Table 1) was constructed by ligation of p9C with p23a as follows. The 5′-end of p23a was phosphorylated by T4 polynucleotide kinase and ATP. A mixture of p9C, p23a, and p23b (3 nmol each) in 250 μl of a buffer containing 5 mM Tris-HCl, 0.5 mM EDTA, 50 mM NaCl, pH 8.0, was denatured for 5 min at 95 °C, incubated for 10 min at 60 °C, and then cooled slowly to form the partial duplex structure of these three oligonucleotides (supplemental Fig. S1). The sample of the duplex oligonucleotide was mixed with 190 μl of Milli-Q water and 50 μl of ×10 ligation buffer (500 mM Tris-HCl (pH 7.5), 100 mM $MgCl_2$, 100 mM DTT, 10 mM ATP). Ligation was initiated by adding 10 μl of T4 DNA ligase (4,000 units), and the mixture was then incubated for 20 h at 16 °C. An additional incubation at 37 °C for 60 min was carried out after the addition of 1 μl of T4 DNA ligase, and the reaction was stopped by further incubation at 68 °C for 10 min. The p32C was separated by 18% PAGE containing 8 M urea, and excised and eluted as described previously (28). p32B and p32D were constructed using a similar method as for p9B and p9D, respectively (see Table 1). The purities of these oligonucleotides, p32B, p32C, and p32D, were determined by denatured PAGE after 5′-end labeling and UV absorbance at 260 and 370 nm.

Primer oligonucleotides were labeled with ^{32}P at the 5′-end as described previously (29), and then purified by MicroSpin™ G-25 or G-50 columns (GE Healthcare) as recommended by the supplier. The mixture of template and labeled primer (50 pmol each) in 400 μl of a buffer containing 8 mM Tris-HCl, 0.8 mM EDTA, 150 mM KCl (pH 8.0) was heated at 70 °C for 7 min, and then cooled slowly to room temperature. In the case of the substrates for TLS polymerases, pol η, pol ι, pol κ, and REV1, the final concentrations of template-primer and the constituents of the annealing buffers were changed to 500 nM and 10 mM Tris-HCl, 1 mM EDTA, and 50 mM NaCl (pH 8.0), respectively.

In Vitro DNA Synthesis Assay—A primer extension reaction was performed as described previously (30) with some modifications. Briefly, an aliquot of 0.75 μl of this primer-annealed template (final concentration, 12.5 nM) was mixed with 0.75 μl of ×10 Klenow buffer (100 mM Tris-HCl (pH 7.5), 70 mM $MgCl_2$, 1 mM DTT), 0.5 μl of 500 mM KCl, 0.5 μl of dNTP mixture (50 μM each), and 4.5 μl of Milli-Q water. After addition of 0.5 μl of Klenow fragment, the mixture was incubated at 37 °C for 10 min. The reaction was terminated by adding 1.5 μl of stop solution (160 mM EDTA, 0.7% SDS, 6 mg/ml proteinase K), and the samples were incubated at 37 °C for 30 min. Subsequently, 5.5 μl of the gel loading solution (30 mM EDTA, 0.05% bromophenol blue, 0.05% xylene cyanol, 97% formamide) was added to the samples. For pol δ, a ×10 reaction buffer containing 200 mM PIPES (pH 6.8), 20 mM $MgCl_2$, 10 mM 2-mercaptethanol, 200 μg/ml bovine serum albumin, and 50% glycerol was used instead of the buffer described above, and the reaction was carried out at 37 °C for 10 min. For other DNA polymerases, pol α, pol I, r*Taq*, and *Tth*, the constituent of each ×10 reaction buffer was altered as recommended by the suppliers.

The reaction using pol κ was performed as described above with some modifications. Briefly, an aliquot of 0.5 μl of this primer-annealed template (final 50 nM) was mixed with 0.5 μl of 10 × TLS buffer (250 mM Tris-HCl (pH 7.0), 50 mM $MgCl_2$, 50 mM DTT, 1 mg/ml bovine serum albumin), 0.5 μl of dNTP solution, and 3.0 μl of Milli-Q water. After addition of 0.5 μl of pol κ, the mixture was incubated at 30 °C for 20 min. The reac-

tion was terminated by adding 8.8 μl of the gel loading solution and a further incubation at 95 °C for 3 min. The reaction of REV1 was performed in the same manner as the reaction of pol κ with the exception that the standard reaction time was 5 min. For pol η, a ×10 reaction buffer containing 400 mM Tris-HCl (pH 8.0), 10 mM $MgCl_2$, 100 mM DTT, 1 mg/ml bovine serum albumin, and 450 mM KCl was used instead of the ×10 TLS buffer. The ^{32}P-labeled fragments were denatured and electrophoresed in a 9.5% polyacrylamide gel containing 8 M urea. The radioactivity of the fragments was determined using a Bio-Imaging Analyzer (BAS2500, Fuji Photo Film, Kanagawa, Japan). Kinetic parameters were determined by steady-state gel kinetic assays under similar conditions as described above. The incubation time for pol κ was changed to 10 min. K_m and k_{cat} were evaluated from the plot of the initial velocity *versus* the dCTP or dGTP concentration using a hyperbolic curve-fitting program in SigmaPlot 11 (Systat Software, Inc.). Data from two or three independent experiments were plotted together.

RESULTS

Construction of Template Oligonucleotides Containing a PhIP Adduct—We designed oligonucleotides containing a dG-C8-PhIP adduct at specific sites for use as templates in *in vitro* DNA synthesis analyses. For this purpose, we selected the 5′-TCCGGGAAC-3′ sequence as: 1) it corresponds to codon 868–870 of the rat *Apc* gene, one of three mutation hot spots (a single base deletion of G) in PhIP-induced colon tumors (21), and could thus be used as a model template that would reconstitute mutations of this gene; 2) two other mutation hot spots in the rat *Apc* gene and many mutated sites induced by PhIP in cultured cells and animal models contain 5′-GGGA-3′ as a core sequence (17–20). We thus speculated that the 5′-TCCGGGAAC-3′ sequence could be used as a model sequence for these GGGA to GGA mutations to some extent; and 3) some mutagenic compounds forming dG adducts, including PhIP, are expected to react preferentially with the 5′-G of a GG dinucleotide site when compared with a single G residue (31). We thus selected a sequence containing GGG as a template for our initial analysis.

We have recently synthesized three 9-mer oligonucleotides separately harboring a PhIP adduct on each G within the sequence 5′-TCC GGG AAC-3′ (22). Three 32-mer template oligonucleotides, p32B, p32C, and p32D, were constructed in our present study by ligation of these 9-mer oligonucleotides containing the dG-PhIP adduct with a 23-mer oligonucleotide, p23a, (Table 1 and supplemental Fig. S1). The purities of these oligonucleotides were tested after resolution by electrophoresis. In our present study, we principally describe the results of our *in vitro* DNA synthesis analysis using p32C as the template to avoid complexity.

In Vitro DNA Synthesis by A- and B-family DNA Polymerase—Many of the chemical compounds that can form DNA adducts *in vivo* and that show mutagenicity have been reported to impede the progress of DNA synthesis to different extents. The molecular size of PhIP is greater than most other mutagenic chemicals that form adducts. Hence, dG-PhIP was expected to block DNA synthesis to a considerable extent. To examine the effects of the dG-C8-PhIP adduct upon DNA synthesis, primer

TABLE 1
Oligonucleotide templates and primers

Oligonucleotide	Sequence[a]
p32A	5′-TCC GGG AAC TGACTCGTC GTGACTGGG AAAAC-3′
p32B	5′-TCC **G**GG AAC TGACTCGTC GTGACTGGG AAAAC-3′
p32C	5′-TCC G**G**G AAC TGACTCGTC GTGACTGGG AAAAC-3′
p32D	5′-TCC GG**G** AAC TGACTCGTC GTGACTGGG AAAAC-3′
p29	5′-GTT TTC CCA GTCACGACG AGTCAGTTC CC-3′
p28	5′-GTT TTC CCA GTCACGACG AGTCAGTTC C-3′
p27	5′-GTT TTC CCA GTCACGACG AGTCAGTTC-3′
p26	5′-GTT TTC CCA GTCACGACG AGTCAGTT-3′
p22	5′-GTT TTC CCA GTCACGACG AGTC-3′
p17	5′-GTT TTC CCA GTCACGAC-3′

[a] The bold G indicates the site of the PhIP-C8-dG adduct. Underlined sequences correspond to codon 868–870 at nucleotides 2602–2610 of the rat APC gene.

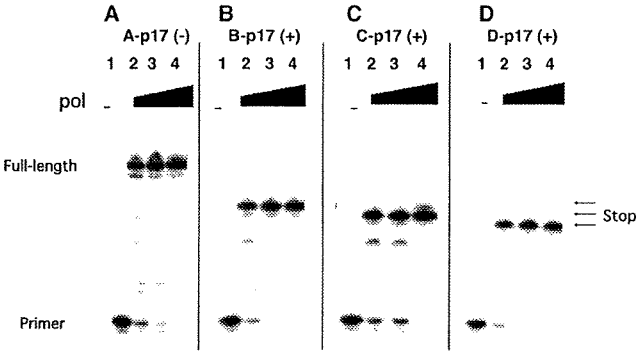

FIGURE 2. ***In vitro* DNA synthesis using Klenow fragment.** Gel electrophoresis indicating the primer extensions obtained using the 32-mer oligonucleotide templates, p32A (*A*), p32B (*B*), p32C (*C*), and p32D (*D*), which have no PhIP adduct, and a PhIP adduct on the first, second, and third G within the triple G sequence, respectively. The 3′ complementary 17-mer sequence, p17, was used as the extension primer. The final concentration of each template-primer complex was 12.5 nM. Concentrations of Klenow fragment were 0 (*lane 1*), 7.8 (*lane 2*), 23 (*lane 3*), and 78 units/ml (*lane 4*).

extension experiments using p32B, p32C, and p32D as templates were carried out (see Table 1). The length of each produced fragment was precisely determined using ladders of oligonucleotide fragments as markers (data not shown). The Klenow fragment of *E. coli* DNA polymerase I, a member of the A-family DNA polymerases, was first used in this analysis. The production of a 28-, 27-, and 26-mer from these primer extension reactions using B-p17, C-p17, and D-p17, respectively, using a template-primer complex, and lack of longer fragments indicated that the Klenow fragment stalled just before the dG-C8-PhIP adduct (Fig. 2). On the other hand, control experiments using p32A without the adduct as a template produced a 32-mer fragment (Fig. 2*A*). Similar results were obtained with *E. coli* DNA polymerase I (exo^+) and B-family DNA polymerases, such as the thermophilic bacterial DNA polymerases, r*Taq* and *Tth*, and human DNA polymerase α (data not shown) (supplemental Fig. S2), suggesting that stalling at the dG-C8-PhIP adduct occurs for all replicative DNA polymerases. Stalling of r*Taq* and *Tth* at the PhIP adduct was observed at 65 °C, as well as at 37 °C, indicating that this is the result of a physical hindrance of the adduct itself and not from secondary DNA structures. Moreover, there was no difference found between the stalling of *E. coli* DNA polymerase I (exo^+) and that of the Klenow fragment (exo^-). This indicates that the physical blocking of DNA polymerases at the dG-C8-PhIP adduct does not depend upon their proofreading function.

Finally, DNA synthesis analyses with human DNA polymerase δ (pol δ), a member of the B-family DNA polymerases and a truly replicative polymerase, were carried out. In the case of using p32C and p17 (C-p17) as a template-primer complex, the production of 27-mer fragments indicated the stalling of pol δ just before the PhIP adduct (Fig. 3, *lane 11*). From a control reaction using A-p17, a template-primer complex without the PhIP adduct, a full-length product of 32-mer was generated (Fig. 3, *lane 8*). In addition to these major products, minor products extended one nucleotide further (28- and 33-mer) and ladders of bands indicating degradation of primer (<17-mer) were observed (Fig. 3), corresponding with previous results reporting terminal dA transferase and exonuclease activities of pol δ (32). PCNA, an accessory protein acting as a sliding clamp for pol δ, was previously reported to promote DNA synthesis by pol δ past several template lesions, including abasic sites, 8-oxo-dG, and aminofluorene-dG (32). In the case of dG-C8-PhIP, however, PCNA was unable to promote the bypass synthesis of pol δ beyond the lesion (Fig. 3, *lane 12*). Extension reaction from the longer 22-mer primer, p22, also paused completely just before the PhIP adduct in the presence or absence of PCNA (Fig. 3, *lanes 5* and *6*). These results strongly suggest that the dG-C8-PhIP adduct on genome DNA in the living cells induces the complete block of replication forks including pol δ, PCNA, and pol α.

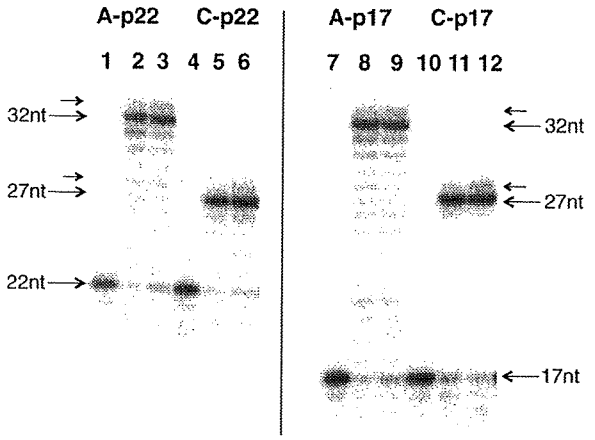

FIGURE 3. ***In vitro* DNA synthesis using pol δ in the presence or absence of PCNA.** Gel electrophoresis indicating the primer extensions obtained using the 32-mer oligonucleotide templates, p32A (*A*), and p32C (*C*), which have no PhIP adduct, and a PhIP adduct on the second G within the triple G sequence, respectively. The 3′ complementary 22- and 17-mer sequences, p22 and p17, were used as the extension primer. The final concentration of each template-primer complex was 12.5 nM. Concentrations of pol δ were 0 (*lanes 1, 4, 7,* and *10*) and 16 nM (*lanes 2, 3, 5, 6, 8, 9, 11,* and *12*). Concentrations of PCNA as a trimer were 0 (*lanes 1, 2, 4, 5, 7, 8, 10,* and *11*) and 20 nM (*lanes 3, 6, 9,* and *12*). *Large arrows* indicate the positions of primers (17- or 22-mer), full-length products (32-mer), and the products pausing just before the PhIP adduct (27-mer). *Small arrows* indicate the minor products that incorporated an additional 1 nucleotide (*nt*) to a full-length product or the pausing product.

Translesional DNA Synthesis by Y-family DNA Polymerases—Translesional DNA synthesis at the dG-C8-PhIP adduct by the Y-family DNA polymerases, pol η, pol κ, pol ι, and REV1 was next examined. Two substrates, C-p27 and C-p28, and their counterparts without a PhIP adduct, A-p27 and A-p28, were used in these experiments (Fig. 4). Substrate C-p27 was prepared by annealing the p32C template (see Table 1) to its 3′-complimentary 27-mer sequence, p27, and was used to identify the nucleotides that are inserted opposite the dG-C8-PhIP adduct (Fig. 4). Similarly, substrate C-p28 was used to analyze the extension reaction from the 3′-end of the dC bases opposite the dG-C8-PhIP adduct (Fig. 4). We found that recombinant human DNA polymerase η (pol η) could insert a dC opposite the dG-C8-PhIP adduct, although at low efficiency compared with control experiments without the PhIP adduct (Fig. 5, *A* and *B*). Extension reactions catalyzed by pol η from the 3′-end of dC opposite the adduct were barely detectable (Fig. 5*D*), although an excessive amount of pol η produced byproducts that incorporated a mismatch nucleotide, dG, dA, or dT (supplemental Fig. S4). In the case of dG, incorporation of one to three dG nucleotides was observed (supplemental Fig. S4). In control experiments without the PhIP adduct, minor products were produced that incorporated mismatch nucleotides, in addition to a major product that incorporated a dC (Fig. 5*C*).

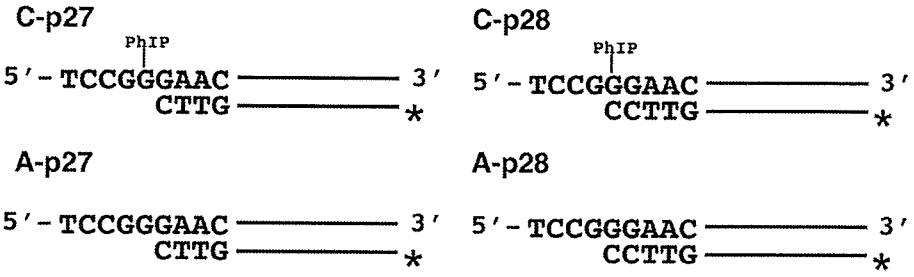

FIGURE 4. **Template-primer complexes.** Substrates C-p27 and C-p28 (series-C) have a PhIP adduct on the second dG within a GGG sequence. Substrates A-p27 and A-p28 (series-A) are control substrates without a PhIP adduct. The corresponding 3′ complimentary 27- and 28-mer sequences, p27 and p28, were used as extension primers. The template-primer complexes, C-p27 and C-p28, were used to monitor the nucleotide insertions into the site opposite dG-C8-PhIP and the extension reactions from the 3′-dC opposite dG-C8-PhIP, respectively.

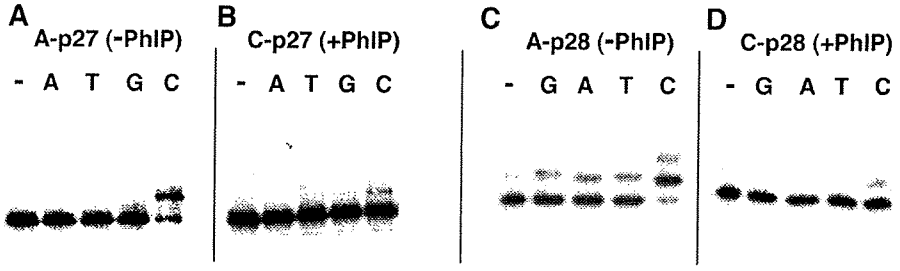

FIGURE 5. **Translesional DNA synthesis by pol η using substrates C-p27 and C-p28.** Control reactions were performed using substrates without the PhIP adduct, A-p27 (*A*) and A-p28 (*C*). An insertion reaction was performed with substrate C-p27 (*B*) and an extension reaction with substrate C-p28 (*D*). A single dNTP (G, A, T, C) was added into the reaction mixture as indicated by *G, A, T,* and *C above* each lane. The lanes indicated by – are controls without any nucleotides. Concentrations of pol η and each dNTP were 1.9 nM and 100 μM, respectively.

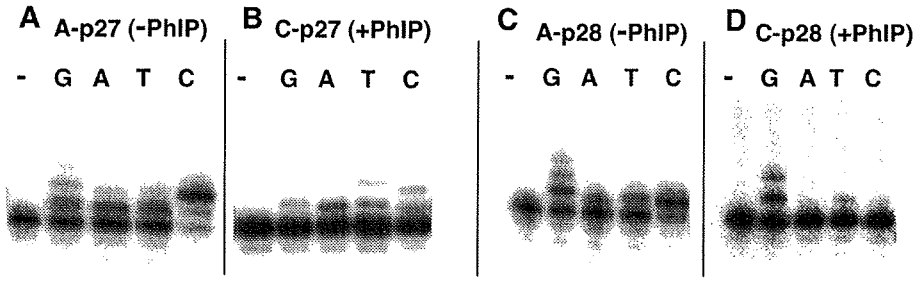

FIGURE 6. **Translesional DNA synthesis by pol κ using substrates C-p27 and C-p28.** Control reactions were performed using substrates without the PhIP adduct, A-p27 (*A*) and A-p28 (*C*). An insertion reaction was performed with substrate C-p27 (*B*) and an extension reaction with substrate C-p28 (*D*). A single dNTP (G, A, T, C) was added into the reaction mixture as indicated by *G, A, T,* and *C above* each lane. The lanes indicated by − are controls without any nucleotides. The concentrations of pol κ were 250 (*A* and *C*), 500 (*B*), and 1000 nM (*D*), respectively. The concentration of each dNTP was 100 μM.

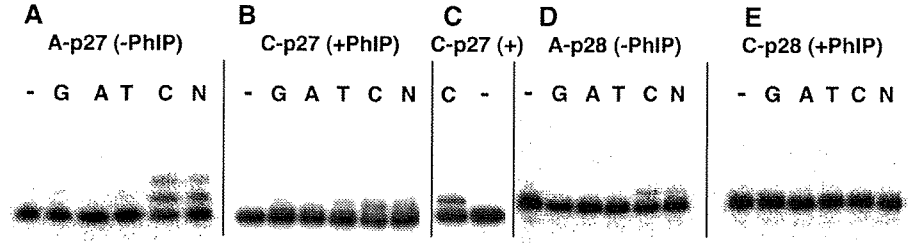

FIGURE 7. **Translesional DNA synthesis by REV1 using substrates C-p27 and C-p28.** Control reactions were performed using substrates without the PhIP adduct, A-p27 (*A*) and A-p28 (*D*). Insertion reactions were performed with substrate C-p27 (*B* and *C*) and an extension reaction with substrate C-p28 (*E*). A single dNTP (G, A, T, and C) or a mixture of each was added into the reaction mixture as indicated by *G, A, T, C,* and *N above* each lane. The lanes indicated by − are controls without any nucleotides. The concentrations of REV1 were 5.2 (*A* and *D*) and 26 nM (*B, C,* and *E*), respectively. The concentrations of each dNTP were 100 μM (*A, B, D,* and *E*) and 320 μM (*C*), respectively. The *N* mixture contained each dNTP at a concentration of 25 μM.

We next examined translesional DNA synthesis beyond the PhIP adduct using a truncated form of human DNA polymerase κ containing the N-terminal 559 amino acids. One or two dCs were inserted opposite the dG-C8-PhIP adduct by this polymerase, and misinsertions of three other nucleotides were also observed to a certain extent (Fig. 6*B*). pol κ incorporated two dCs and misincorporated dG, dA, and dT into the A-p27 substrate without the PhIP adduct at a low efficiency (Fig. 6*A*). Misincorporations of dG, dA, and dT into the A-p28 substrate without the adduct were also observed (Fig. 6*C*). In the case of the extension reaction from 3′-dC opposite the dG-PhIP adduct, pol κ also incorporated dC and misincorporated dT into the C-p28 substrate at low efficiency (Fig. 6*D*). Interestingly, one- and two-base incorporations of dG into the substrate C-p28 by pol κ dominated the incorporation of a dC (Fig. 6*D*). In the extension reaction with pol κ in the presence of all four dNTPs, fragments of 29 and 30 nucleotides were observed as major products, and a small amount of the 31-nucleotide fragment was observed (see supplemental Fig. S5, *lane 6*). Full-length products of 32 nucleotides were observed only when an excess amount of pol κ was present (data not shown). This poor extension activity of pol κ after adding two nucleotides was probably caused by the shortness (~4 nucleotides) of the 5′ region to the lesion in the template oligonucleotide. Extension with pol κ, pol η, and pol δ from the mismatched primers, where the 3′-terminal nucleotide of the p28 primer, dC, was substituted with another nucleotide, could not be observed (data not shown). REV1 inserted a dC opposite the PhIP adduct at a higher efficiency compared with pol κ and pol η (Fig. 7, *B* and *C*). REV1 was, however, unable to catalyze the extension reaction from the dC opposite the PhIP adduct in C-p28 (Fig. 7*E* and supplemental Fig. S5, *lane 5*). REV1 incorporated only dC nucleotides into A-p27 and A-p28 substrates without the adduct (Fig. 7, *A* and *D*). Neither nucleotide insertion nor extension reactions for the templates containing the PhIP adduct were detected using human pol ι (data not shown).

Kinetic Analyses of Translesional DNA Synthesis by pol κ and REV1—To evaluate translesional DNA synthesis beyond the dG-C8-PhIP adduct in further detail, additional quantitative analyses for pol κ and REV1 were performed. Insertion reactions catalyzed by pol κ for dC (Fig. 8, *B, lanes 2–5,* and *C, closed diamonds*) and dG (Fig. 8, *B, lanes 6–9,* and *C, closed triangles*) into substrate C-p28 were analyzed in the same way. Kinetic parameters for pol κ were determined using steady-state kinetic assays (Table 2). The catalytic efficiency (k_{cat}/K_m) of dC insertion into C-p28 (0.039 min^{-1} mM^{-1}) was found to be 4-fold greater than that into C-p27 (0.011 min^{-1} mM^{-1}). These results indicate that pol κ catalyzes the extension reaction from the 3′-terminal of dC opposite the dG-C8-PhIP with a higher efficiency than the insertion reaction opposite the adduct. The k_{cat}/K_m values of the dC insertion opposite the adduct were roughly 4 orders of magnitude less than those into counterparts without the adduct (see Table 2). The k_{cat}/K_m value of the dG incorporation into C-p28 was slightly higher than that of dC, and more than 8-fold higher than that of dG into C-p27 (see Table 2). This result indicates that pol κ skipped over the dG site just 5′ of dG-C8-PhIP on the template and incorporated dG opposite dC on the template strand of substrate C-p28 with a high efficiency. The k_{cat}/K_m values of the dC incorporation into D-p27 (0.19 min^{-1} mM^{-1}) were over 4-fold greater than into C-p28 (0.039 min^{-1} mM^{-1}) and over 8-fold higher than that of dG into B-p29 (0.023) (see supplemental Table S1). These data indicate that the efficiencies of the extension reaction by pol κ are the highest for template p32D containing the PhIP adduct in the third G of the triple G run, next for template p32C containing the PhIP/adduct in the second G, and lowest for template p32B containing the PhIP adduct in the first G.

Even at higher concentrations of dNTPs, extension reactions catalyzed by REV1 for substrate C-p28 could not be monitored (Table 3, Fig. 7*E*). The k_{cat}/K_m value of the dC incorporation by REV1 into substrate C-p27 was more than 2,000 times greater than that by pol k, and 1/44 of the values for counterparts with-

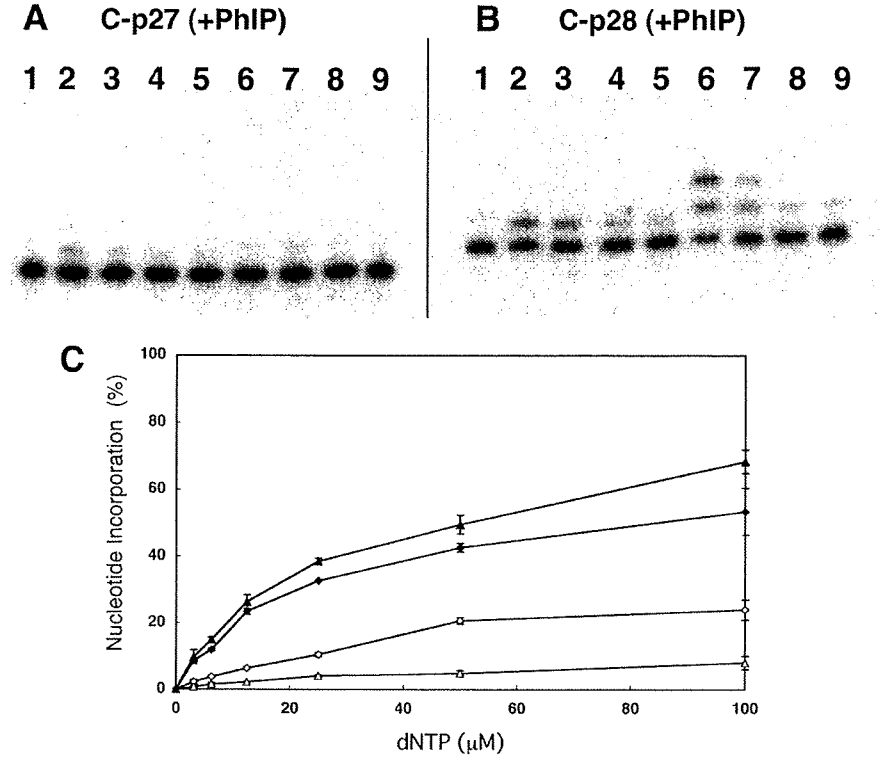

FIGURE 8. **Translesional DNA synthesis by pol κ.** Nucleotide incorporation by pol κ for substrates C-p27 (*A*) and C-p28 (*B*). Either dCTP (*lanes 2-5*) or dGTP (*lanes 6-9*) was added into the reaction mixture. *Lane 1* indicates a control without any nucleotides. The concentration of pol κ was 910 nM. The concentrations of dCTP or dGTP, respectively, were 25 (*lanes 2* and *6*), 12.5 (*lanes 3* and *7*), 6.25 (*lanes 4* and *8*), and 3.13 μM (*lanes 5* and *9*). *C*, incorporation efficiencies of dCTP and dGTP into substrate C-p27 and C-p28. Incorporations of dCTP into C-p27, dGTP into C-p27, dCTP into C-p28, and dGTP into C-p28 are indicated by *open diamonds*, *open triangles*, *closed diamonds*, and *closed triangles*, respectively. Each data point represents the mean of two separate experiments. The *error bars* represent residuals.

TABLE 2
k_{cat}/K_m values for pol κ

Substrate	K_m	k_{cat}	k_{cat}/K_m
	μM	$\times 10^{-3}$ min^{-1}	min^{-1} mM^{-1}
C-p27			
dCTP	70	0.76	0.011
dGTP	47	0.24	0.0050
C-p28			
dCTP	8.0	0.32	0.039
dGTP	11	0.48	0.042
A-p27			
dCTP	0.035	4.4	130
dGTP	0.26	1.3	5.0
A-p28			
dCTP	0.027	3.7	140
dGTP	2.1	8.8	4.1

TABLE 3
k_{cat}/K_m values for dCTP-insertion by REV1

Substrate	K_m	k_{cat}	k_{cat}/K_m
	μM	$\times 10^{-3}$ min^{-1}	min^{-1} mM^{-1}
C-p27	12	320	27
C-p28	ND[a]	ND	ND
A-p27	0.36	390	1100

[a] ND, not detectable.

out the adduct (Table 3). The k_{cat}/K_m values of the dC insertion by REV1 into three substrates, B-p28, C-p27 and D-p26, were 39, 27, and 73 min^{-1} mM^{-1}, respectively. Thus, the insertion reaction catalyzed by REV1 among the three templates was the most efficient for template p32D containing the PhIP adduct at the third G, similar to the extension reaction by pol κ.

DISCUSSION

In Vitro TLS Analysis Reconstituting PhIP-induced Mutations—HCAs are food-borne carcinogens produced when cooking meat (1, 9, 33). The most significant aspect of these molecules is that they exist normally in cooked food and are thus ubiquitous carcinogens (32). The mutagenicity and carcinogenicity of HCAs are mainly attributed to C8- and N2-dG adducts (9). Both excision repair and translesional DNA synthesis play critical roles in the mutagenesis steps induced by HCAs. However, despite the importance of HCAs as common environmental mutagens, there have been very few previous reports regarding the stalling of DNA polymerases and TLS caused by the DNA adducts they form. This is mainly because of the difficulty in preparing template DNA with introduced HCA adducts at specific sites. Choi *et al.* (34) have recently undertaken a biochemical study of TLS at adducts of the HCA 2-amino-3-methylimidazo[4,5-*f*]quinoline (IQ) using purified human polymerases. In our current study of TLS, we describe our findings for adducts of PhIP, the most abundant HCA in cooked foods (4).

A rat colon cancer model induced by PhIP shows profiles of cancer development similar to the multistep model of colon carcinogenesis in humans (35). In this rat model, *p53* and K-*ras* mutations are rarely observed, whereas mutations in *Apc* and its downstream gene *β-catenin* have been frequently observed (21, 36–38). Hence, mutations in *Apc* or *β-catenin* have been speculated to play a critical role in PhIP-induced colon carcinogenesis. Five mutations in the *Apc* gene were previously detected in four of eight PhIP-induced rat colon tumors, and all of these mutations involved a single guanine deletion in the 5′-GGGA-3′ sequence (21). This characteristic mutation induced by PhIP, 5′-GGGA-3′ to 5′-GGA-3′, was also observed in other *in vivo* mutation analyses using transgenic animals harboring introduced reporter genes, such as *lacI* (18–20). Hence, the 5′-TCCGGGAAC-3′ sequence corresponding to a mutation hot spot within the rat *Apc* gene, which we utilized to introduce the PhIP adduct and employed as the template for *in vitro* DNA synthesis analyses, could be a suitable model for revealing the molecular mechanisms associated with PhIP-induced mutations.